# Acknowledgements

I am very grateful to Dr Paul Cosgrove for his expertise and patience in advising on the creation of the Serpent models for this project.

Likewise, I would like to express my thanks to Peter Benie and Jo Boyle for their assistance in setting up the computer access and use of the University HPC.

I am also extremely thankful to my supervisor Professor Geoff Parks for his mentorship and help throughout the project.

Finally, I would like to thank my friends and family for their continuous support.

# Technical Abstract


## Ben Leo Cartman Silva - Emmanuel College


## Modelling the S7G Reactor


The S7G reactor was an experimental reactor developed by General Electric for use in US Navy submarines [14]. In place of using solid control rods that can be inserted and retracted from the core, stationary gadolinium-clad tubes are positioned inside the reactor, and can be filled with varying heights of water. If filled with water, neutrons passing through the tube are moderated, increasing the chance of capture in the gadolinium cladding when exiting the tube, thereby reducing the neutrons available to cause fission in the fissile material. Therefore, reactivity can be increased by lowering the water level in the tubes, or decreased by raising the water level.

By keeping the control tubes in the core, there is no need for a cavity to house control rods when they are retracted, saving valuable space. In civilian power, reducing the size of the reactor brings economic advantages. The pressure vessel height and the size of the hole that must be dug to contain it are two of the principal costs during construction, with the cost of excavation for a deep silo increasing super-linearly with depth [8]. The cost of construction, including the cost of financing the upfront capital loan, heavily influences the economic viability of new nuclear plants, accounting for at least 60% of their Levelised Cost of Electricity [17]. Existing studies have already evaluated technologies such as telescopic control rods in an aim to minimise space [8].

This project builds on a previous 4th year project [6] that evaluated a range of S7G-style fuel lattices. Using the most promising lattice identified in the previous work, this report models a 3D 3-batch core of an S7G reactor using Serpent 2, a Monte Carlo neutron transport code. The fuelled height, power, and number of assemblies are matched against the Rolls-Royce SMR [11], to allow easy comparison with conventional PWR technology. The discharge burn-up of the 3-batch core is found to be 52MWd/kg, which is lower than the Rolls' burn-up of 55-60 MWd/kg, and may be due to the harder neutron spectrum and increased parasitic absorption in the control tube walls. The control worth curve of the control tubes is found to be a highly asymmetric S-curve, with the control worth increasing with water level, unlike the symmetric S-curve of a conventional PWR.

The reactor was evaluated at key operating points, such as hot and cold zero power, and satisfied criticality limits at both start and end-of-cycle. This report details the development of a control tube state algorithm, which is capable of controlling the reactor to $k_{\text{eff}} = 1$ at all points in burn-up, without the use of solube boron, as well as limiting the assembly-wise PPF to be under 1.5 for

45/46 burn-up steps. This is achieved with 113 control tubes operating in a binary fashion, i.e. either 100% water or 100% nitrogen, in order to reduce axial asymmetries in power and burn-up. The remaining 8/121 assemblies operate with a variable control tube level, in order to fine tune $k_{\text{eff}}$ which decreases in a continuous manner.

The control tube algorithm results in the twice-burnt fuel assemblies not using their control tubes for neither reactivity burn-up control nor power peaking management, effectively acting as a shutdown bank. This is pertinent, as a critical design limit for the S7G is the burning up of the control tube gadolinium. The current tube wall thickness results in the tubes burning out during the second fuel cycle if filled with water, leading to an inversion of control gain, as pumping water into the tubes starts to increase the reactor moderation more than it increases absorption in the tube walls. The current model assumes tubes are replaced during refuelling; however, the report also shows that a doubling of the wall thickness results in tubes that can withstand three fuel cycles without burning out, albeit at the expense of increased parasitic absorption and a potential shorter fuel cycle length and lower discharge burn-up.

A second critical design limit has been identified for the S7G, which is the energy deposition directly in the control tube water, by neutron or photon heating. This heating power has the potential to boil the tube water if the water is not circulated sufficiently. Boiling of control tube water would lead to a positive feedback loop, as the control worth of the tubes decreases with the reduction in water level. This report found that the water must be replaced every 6.3 minutes for an average-power assembly in order to avoid boiling.

One aim of this project was to evaluate the suitability of an S7G reactor for load following. In a future energy grid, where nuclear makes up a large share of the energy mix, reactors may be required to vary their power in response to demand, as is already the case in France [9]. However, as load following involves fluctuations in fuel and coolant temperature, over the timescale of many minutes, it was found that a pure neutronics code, such as Serpent, lacked the capability to appropriately simulate the reactor behaviour. Therefore, further research should be directed towards simulating the S7G using a coupled thermal-hydraulics/neutronics code, in order to evaluate transients such as load following and behaviour in accidents. Several accidents, such as loss of coolant and loss of power, were identified as having potentially different responses in the S7G compared to a conventional PWR, due to the novel control mechanism, and these are discussed further in the report.

# Table of contents

# Chapter 1

# Introduction

## 1.1 Background

The S7G reactor was an experimental reactor developed by General Electric for use in US Navy submarines [14]. In place of using solid control rods that can be inserted and retracted from the core, stationary gadolinium-clad tubes are positioned inside the reactor, and can be filled with varying heights of water. If filled with water, neutrons passing through the tube are moderated, increasing the chance of capture in the gadolinium cladding when exiting the tube, thereby reducing the neutrons available to cause fission in the fissile material. Therefore, reactivity can be increased by lowering the water level in the tubes, or decreased by raising the water level.

In submarines, the advantage of an S7G reactor is clear. By keeping the control tubes in the core, there is no need for a cavity to house control rods when they are retracted, saving valuable space. In civilian power, reducing the size of the reactor also brings advantages. The pressure vessel height, and the size of the hole that must be dug to contain it, are two of the principal costs during construction, with the cost of excavation for a deep silo increasing super-linearly with depth [8]. The cost of construction, including the costs of financing the upfront capital loan, heavily influence the economic viability of new nuclear plants, accounting for at least 60% of their levelised cost of electricity [17]. Existing studies have already evaluated technologies such as telescopic control rods in an aim to minimise space [8].

In conventional Pressurised Water Reactors (PWRs), control rods are used for shutdown and startup, with soluble boron being used to provide fine whole core control. Boron, a very high neutron absorber, is dissolved in the moderator, and the concentration is then gradually reduced over the length of the fuel cycle, as the reactivity of the fuel decreases, reaching zero just before refuelling. The use of soluble boron is a significant cost in existing PWRs. The cost and space requirements for the boron control equipment remains relatively fixed as the volume or power of the reactor varies, meaning that for a Small Modular Reactor (SMR) with a lower rated power, the contribution due to boron to the cost per kilowatt/hour is higher than for a conventional PWR. Therefore one way to reduce the cost of an SMR is to not use soluble boron, such as in the Rolls-Royce SMR [11].

Currently, nuclear reactors in the UK operate as a baseload provider, meaning they run at full rated power all of the time (except during refuelling), and other sources of power such as gas turbines and hydroelectric plants vary their power as needed to match demand. In the event of widespread construction of SMRs across the UK, nuclear plants would make up a larger proportion of the energy mix and may need to vary their power output in a response to demand as well, this is called 'load following'. This is already the case in countries with a large share of nuclear power, such as France [9]. Load following complicates the control logic necessary in a reactor, and necessitates a control system that is robust and fast enough to respond routinely to transients in power level.

## 1.2 Previous Work

Due to the military nature of the reactor, technical details and models of S7G reactors are extremely limited in the public domain. The most significant public research is the MEng project report by Jack Lawrence [6], which investigated a range of potential lattices in order to evaluate their performance and suitability for use in a reactor. The project used a conventional PWR lattice as its base design (17×17 fuel pins, clad with Zircaloy-4) and replaced some pins with control tubes. The report found that to achieve a sufficient $\Delta k_{\text{eff}}$ (effective multiplication factor) between the 100% nitrogen and 100% water states to shut down the fission process at any stage, it was necessary to replace a large fraction of pins with control tubes (15.6%). In order to counter-act the reduction in fuel pins, a higher enriched uranium dioxide fuel was recommended with an enrichment level of 9.2% as opposed to the 3.5-5% commonly used by PWRs [19]. The best lattice found is displayed in Figure 1.1, with the dimensions shown in Table 1.1. 8 of the 9 control tubes in the lattice lie on the lattice boundary, meaning the tubes are only sealed via the tessellation of multiple assemblies.

The previous work found that the neutron spectrum of an S7G lattice is harder than an equivalent PWR lattice, meaning there are fewer thermal neutrons, particularly when the control tubes are filled with nitrogen. The work also found that the control tube thickness is a critical design limit for the S7G, as at extended cycle lengths, the gadolinium may burn out, and become unable to provide effective control. The tube gadolinium composition is $Gd_2O_3$ with a density of $7.41\text{g/cm}^3$.

The previous work had used the WIMS code [1] to quickly test lattice designs, and the SERPENT 2 [7] code to confirm the results. WIMS is a deterministic neutron solver, which is quicker but less accurate than the Monte Carlo particle transport code SERPENT 2.

## 1.3 Project Aims

- Convert the existing 2D lattice from the previous project to a 3D assembly, by fixing key assembly design points

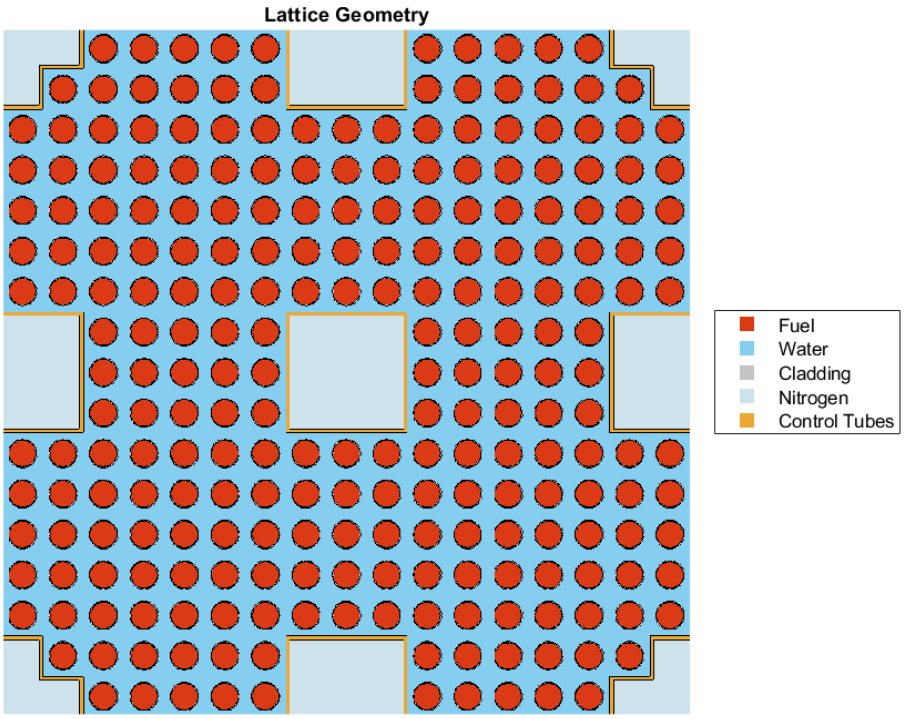


Fig. 1.1 Best fuel lattice found in previous work

| Part | Size (cm) |
|---|---|
| Lattice side length | 21.42 |
| Lattice pitch | 1.26 |
| Control tube thickness | 0.12 |
| Outer radius of fuel in pin | 0.4096 |
| Outer radius of helium gap | 0.4138 |
| Outer radius of Zircaloy-4 cladding | 0.4423 |

Table 1.1 Lattice dimensions

- Create a 3D mock-up of the S7G reactor using batch refuelling, ensuring an appropriate $k_{\text{eff}}$ at all relevant design points
- Control power peaking via the use of burnable poisons and fuel loading patterns
- Design control logic that can fine tune $k_{\text{eff}} = 1$ at all stages of burn-up without the need for soluble boron
- Study the suitability of the control system for load following

As the design of a reactor is an open problem, the design specifications of the Rolls-Royce SMR, detailed in the technical report [11], will be used to aid the design of the S7G core, for example by fixing the rated power and core dimensions, to allow comparison between the control tubes and conventional rods. The design of the fuel lattice will be taken from the previous work, using the best lattice found, shown in Figure 1.1. As this project will deal only with 3D cases, all simulations will be conducted using SERPENT 2, as for 3D applications, WIMS lacks the capability to capture many of the more complex phenomena. The version of Serpent used was 2.1.31, and the cross-section data used in simulations was JEFF31, except where specified.

# Chapter 2

# 2D-3D Lattice Conversion

## 2.1 Height of Fuel Pins

The height of the fuel pin affects the effective multiplication factor ($k_{\text{eff}}$) value. Varying the height of the fuel pin varies the aspect ratio of the lattice (for a fixed width), as the aspect ratio becomes further from 1:1, the surface area to volume ratio increases. This results in increased neutron leakage, which decreases the reactivity. For an infinite lattice, raising the height of the fuel pin always decreases the surface area to volume ratio. Figure 2.1 shows the variation in $k_{\text{eff}}$ with the height of the fuel pin. The simulation assumes a lattice infinite in the x-y plane by imposing reflective boundary conditions at the sides, and places a vacuum boundary condition at the top and bottom. The figure shows that the $k_{\text{eff}}$ value increases linearly with height, up until around 1.5m where the variation levels out. At 10m, the $k_{\text{eff}}$ value for the nitrogen case is around 0.1 below the infinite lattice, and for the water case it is about 0.04 below. This means that the $\Delta k_{\text{eff}}$, or the maximum control possible, is reduced slightly for the real system. We can also see that, in the region of 2-10m, the $\Delta k_{\text{eff}}$ increases with height.

Typical PWR fuel pins are between 4-5m in height [18], so for a Small Modular Reactor of perhaps 1/3 power output of a PWR, we would expect the fuel pin to be smaller. To allow easy comparison with the Rolls-Royce SMR, the height of the fuel pin was fixed at 2.8m.

### 2.1.1 Choice of Simulation Settings (Shannon Entropy)

Monte Carlo simulations such as those conducted using Serpent are random in nature, meaning many neutron histories need to be simulated in order for the average behaviour to be estimated. However, in order to initialise the x-y-z coordinates of a neutron, an initial guess on the distribution of neutrons inside the reactor is needed, as picking random coordinates would assume a spatially uniform neutron flux. To find the spatial distribution of neutrons, Serpent runs a number of ‘inactive cycles’, which are used to converge on a neutron distribution, but whose results are not used when averaging the simulation results. A number of ‘active cycles’ are then used to average the simulation results. The number of active/inactive cycles, along with the

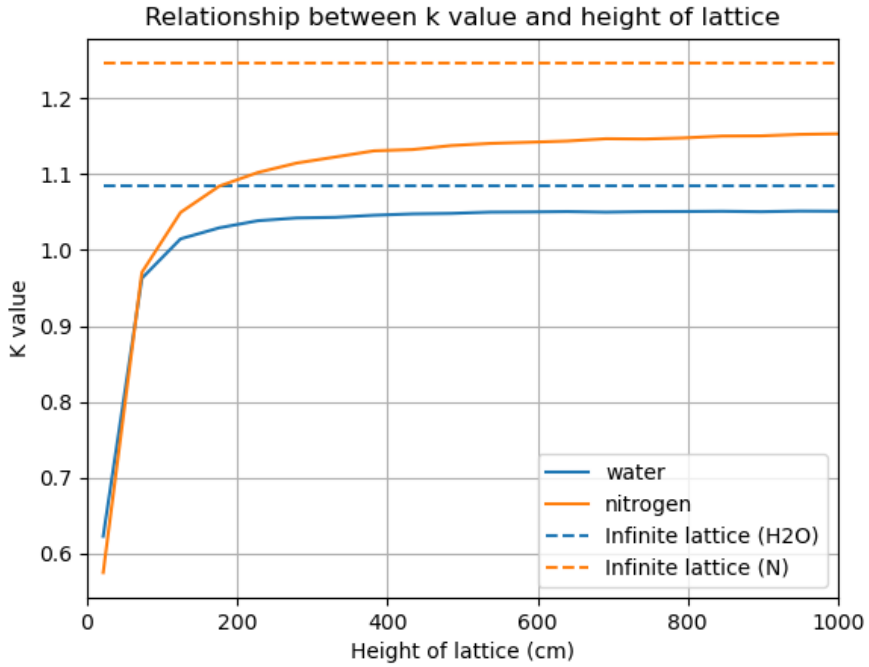


Fig. 2.1 Variation of $k_{\text{eff}}$ with lattice height for nitrogen and water-filled control tubes *10000 neutrons per generation, 100/50 active/inactive cycles, error* $1E-3$

number of neutrons in each generation (cycle) are reported under each graph of results, along with the corresponding error, which is expected to decrease with increasing active cycles and neutron histories. To calculate the appropriate number of inactive cycles needed to converge, the model was split into 10 zones along the z-axis (the largest dimension), and the evolution of the cycle-wise Shannon Entropy was calculated, the results of which are shown in Figure 2.2. The figure shows that up to 100 cycles there is significant change in the Shannon Entropy, suggesting that the neutron distribution has not converged. Therefore at least 100 inactive cycles were used for the simulations.

## 2.2 Height of Axial Reflector

To minimise neutron leakage, reactors are surrounded by axial and radial reflectors. The reflector reflects neutrons that would otherwise escape and therefore affects the $k_{\text{eff}}$ value. Using a reflector also increases fuel utilisation at the periphery, making the core power distribution more uniform. Common reflector materials include graphite, beryllium, water, and natural uranium [15]. For the purposes of a neutronics simulation, and for research reactors, a pool of water is sufficient for both the axial and radial reflectors, therefore it will be used for simplicity of the model. Figure 2.3 shows the variation of $k_{\text{eff}}$ with the height of the water axial reflector. The figure shows that beyond a height of 10cm, there is minimal variation in $k_{\text{eff}}$ for either max or min control scenarios. Therefore, to reduce the size of the model, the height of the axial reflector was fixed at 25cm.

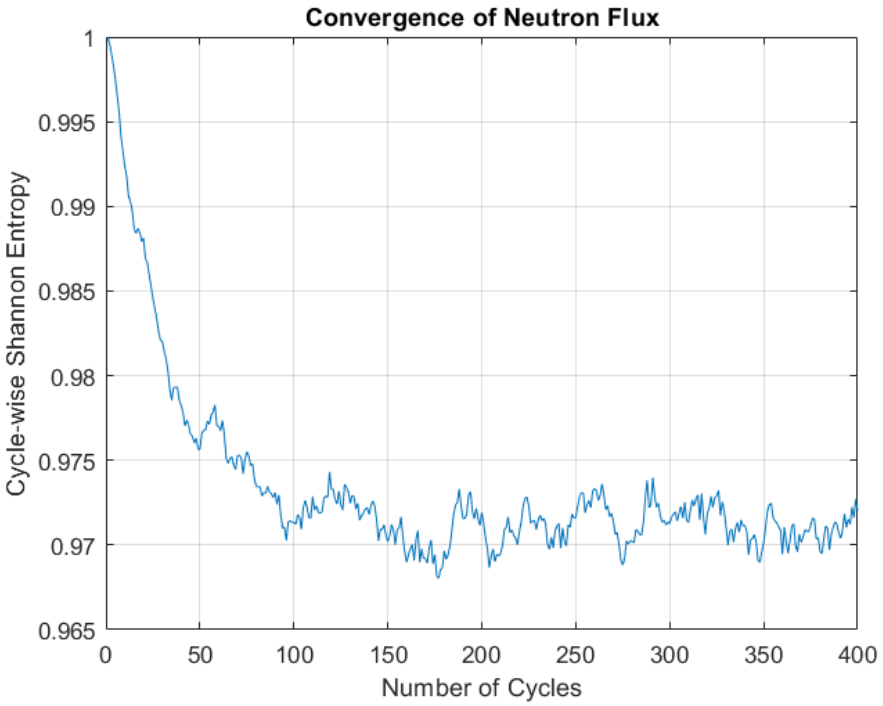


Fig. 2.2 Variation of Shannon Entropy with number of cycles for a nitrogen filled 2.8m assembly

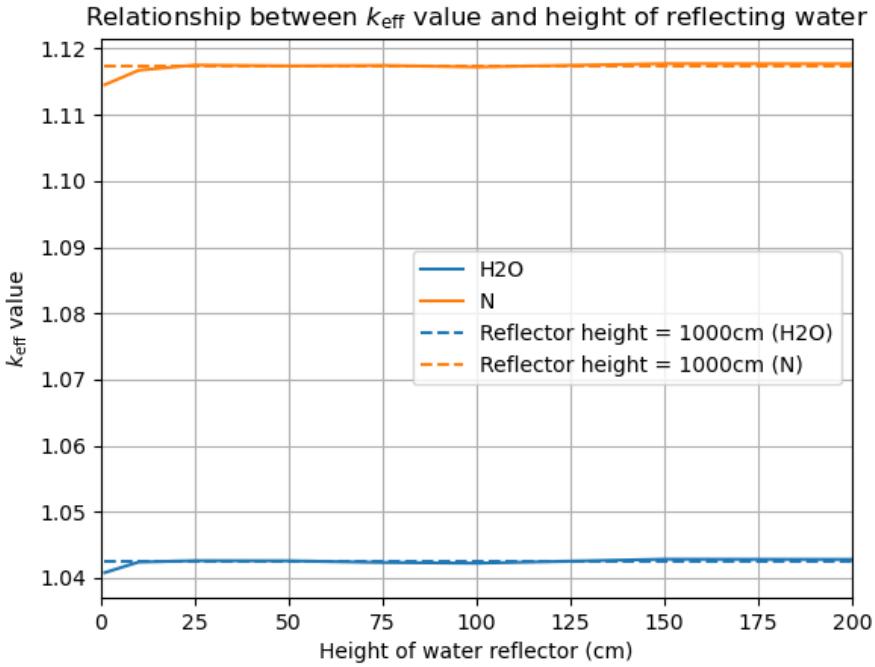


Fig. 2.3 Variation of $k_{\text{eff}}$ with height of axial reflector
*10000 neutrons per generation, 1000/100 active/inactive cycles, error* $2E-4$

## 2.3 Single Lattice Fuel Burn-Up

As the fuel undergoes fission, the $k_{\text{eff}}$ decreases due to several factors such as:

- The build-up of fission products including xenon-135, which have high neutron absorption cross-sections
- The reduction in number of fissile atoms, as U-235 is removed via fission
- The changing of the neutron spectrum, as fertile isotopes are transmuted into different fissile isotopes such as Pu-239, they become significant contributors to fission events

When $k_{\text{eff}}$ goes below 1, the fission chain reaction can no longer sustain itself, and rated power can no longer be maintained, leading to reactor shutdown. The length of time (at a given power) that it takes for the $k_{\text{eff}}$ to reduce to 1 is therefore important, as it dictates how long the fuel can remain in the reactor and produce energy. We can measure this burn-up in Effective Full Power Days (EFPD), i.e. how many days at the rated reactor power has the fuel been exposed to. One way of extending fuel burn-up is to use a batch reloading scheme. The behaviour of a batch loaded core can be approximated using the Partial Reactivity Model (PRM) [3] which approximates the total core reactivity as the mass-weighted sum of the reactivities of the different fuel assemblies in the core. In this way, a core composed half of fuel with $k_{\text{eff}} = 1.1$ and half with $k_{\text{eff}} = 0.9$ will have a total multiplication factor of $k_{\text{eff}} = 1$, allowing a chain reaction to be sustained. This means that energy can continue to be extracted from sub-critical fuel, reducing the amount of fresh fuel needed, and decreasing the volume of fuel waste for the same energy produced. Mixing super-critical fuel with sub-critical fuel also reduces the amount of reactivity control needed, as the sub-critical fuel absorbs the excess neutrons emitted by the super-critical fuel.

In order to take advantage of this effect, most PWRs including the Rolls-Royce SMR use a 3-batch system [11]. The first batch is fresh, unburnt fuel. According to the PRM, the third batch has an initial value of $k_{\text{eff}} = 1$ (in reality there will be variation between each assembly within the same batch), and the second batch has a burn-up level equal to half that of the third batch. When the Partial Reactivity Model is combined with the Linear Reactivity Model, which states that the variation of $k_{\text{eff}}$ with burn up is approximately linear, the average $k_{\text{eff}}$ for the whole core is therefore equal to $k_{\text{eff}}$ of the second batch, as the $\Delta k_{\text{eff}}$ between the second and the first and third batches are equal in magnitude but opposite in sign. To calculate the irradiation corresponding to a full power day, the power per lattice is taken from the Rolls SMR specification. The SMR has a rated electrical output of 470MW. Assuming a whole cycle efficiency of 33% [19], this gives a core power of 1410MW, or 11.65MW per fuel assembly for a core composed of 121 assemblies. As the burn-up calculation is conducted on an x-y infinite lattice, it does not account for radial neutron leakage, hence we assume 3% neutron leakage, and propose that the fuel becomes sub-critical when $k_{\text{eff}} = 1.03$.

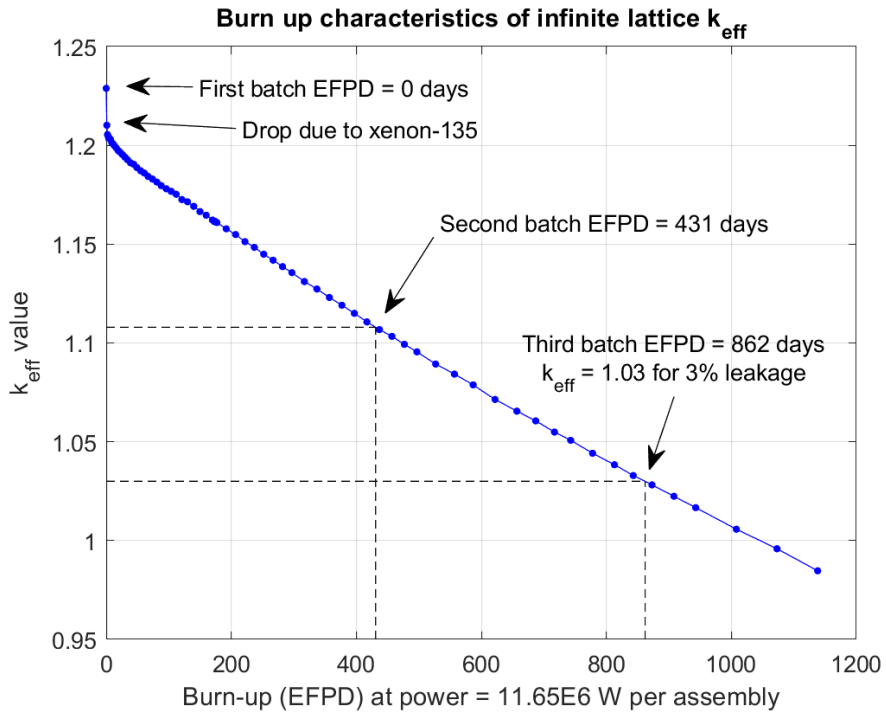


Fig. 2.4 Variation of $k_{\text{eff}}$ with burn-up (No axial discretisation or tube burn)
*10000 neutrons per generation, 1000/100 active/inactive cycles, error* $2E-4$

When modelling the burn-up, there are several choices that have to made with regard to the discretisation of burn-up zones. By default, Serpent treats all instances of a material (for example the $UO_2$ fuel) as the same burn-up zone, that means that whilst the material composition of the fuel will vary with burn-up, as fission products are produced, it will remain spatially uniform. This ignores spatial effects, such as that fuel pins closer to control rods are more likely to experience a lower flux, and so experience a slower build-up of fission products. Each individual pin can also be discretised axially, to account for axial flux variations, and non-fuel materials, such as the control tube walls can be set to be burned or not. Adding more burn-up zones increases the accuracy of the model, but also increases the required computational resources, as the memory needed to load the model is proportional to the number of burn-up zones. Therefore, the effect on accuracy should be considered when deciding what burn-up zones to create.

Figure 2.4 shows how the multiplication factor of the S7G lattice varies with burn-up for a basic burn-up zone division model. This divides each pin into a separate burn-up zone, but does not use axial discretisation, nor burn the control tubes. The figure shows that this leads to a cycle length of 431 days. This means that each fuel assembly, when used as part of 3 cycles, will have a total burn-up of 1293 days.

### 2.3.1 Effect of Burning Gadolinium Tubes

Figure 2.5 shows the effect on $k_{\text{eff}}$ of burning the tube gadolinium wall. The figure shows that as the gadolinium burns up, the lattice $k_{\text{eff}}$ increases compared to the non-burn model. This is

because, as the gadolinium burns up, isotopes with a high neutron cross-section will absorb neutrons and be transmuted, lowering the gadolinium average cross-section, and so decreasing neutron absorption. It can also be seen that the tube filled with water burns up faster, which is to be expected, as the tube will absorb more neutrons when filled with water, in order to control the reactivity. Whilst increasing $k_{\text{eff}}$ towards the end of the cycle is usually a positive trait, as it increases the possible cycle length, the figure shows that, due to the different rates of burn-up between the water and nitrogen states, $\Delta k_{\text{eff}}$ decreases markedly at around 800 EFPD (during the assembly's second burn), becoming negative at 900 EFPD. This signifies that the tube wall has burnt out to such an extent that the water in the tube no longer acts as a control method. By filling the burnt-out tube with water, the core moderation is now increased more than the neutron absorption in the tube wall is, leading to a greater $k_{\text{eff}}$ with water in the tubes than with nitrogen. This is clearly an unsafe operating scenario and must be avoided.

As the intention for this project is to design an S7G reactor without using soluble boron, control tubes must be used to balance the initial excess reactivity, meaning that some assemblies will have their tubes filled for the majority of the fuel cycle. This means that there is a significant risk of them burning up and becoming ineffective, as shown in the figure. Whilst the tube walls could be redesigned to have a longer burn life and be able to last 3 fuel cycles, as they were fixed as part of the previous work, this project will not seek to redesign them, and will instead use the existing tube wall thickness of 0.12cm, suggesting that they are replaced at the start of each fuel cycle. However, Figure 2.6 shows that there could be potential for redesigning the tubes in future work, as by doubling the tube thickness, the useful life is extended to last 3 fuel cycles, albeit with a reduction in $k_{\text{eff}}$, which could lead to a shorter fuel cycle. This reduction of $k_{\text{eff}}$ with thickness is around 0.04 for the tubes burnt with water, and 0.05 for the tubes burnt with nitrogen, which would have large effects on cycle length. However, it is not clear to what extent the reduction in $k_{\text{eff}}$ will remain if the tubes are burnt with water, and then filled with nitrogen, as they would be if they were filled with water at the start of cycle, and emptied towards the end.

The tube burn-up curve shown in Figure 2.5 assumes that the assembly operates at core average power with water-filled tubes. In reality this is likely to be an over-estimation, as a whole reactor core will consist of a mix of water-filled and nitrogen-filled assemblies, in order to keep the average $k_{\text{eff}} = 1$. The assemblies filled with water will therefore be expected to have a lower power and neutron flux than the assemblies filled with nitrogen, and so may not operate at the assumed power of 11.65MW, leading to a slower burn-up curve. Inversely, depending on how the control logic is implemented, higher power tubes may be preferentially filled with water, in order to control the power distribution, leading to a faster burn-up. However, it is clear that tube burn-up has a non-negligible effect on core neutronics, including the values of $k_{\text{eff}}$ and $\Delta k_{\text{eff}}$ between the nitrogen and water tube states. Therefore, gadolinium burning must be modelled.

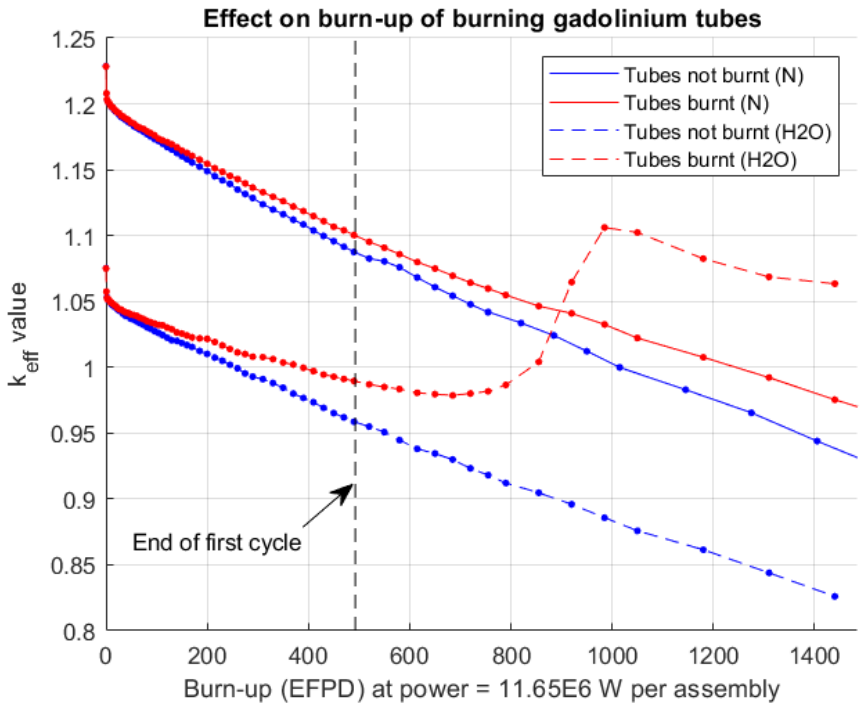


Fig. 2.5 Effect of burning gadolinium tube on burn-up curve
*10000 neutrons per generation, 1000/200 active/inactive cycles, error* $2E-4$

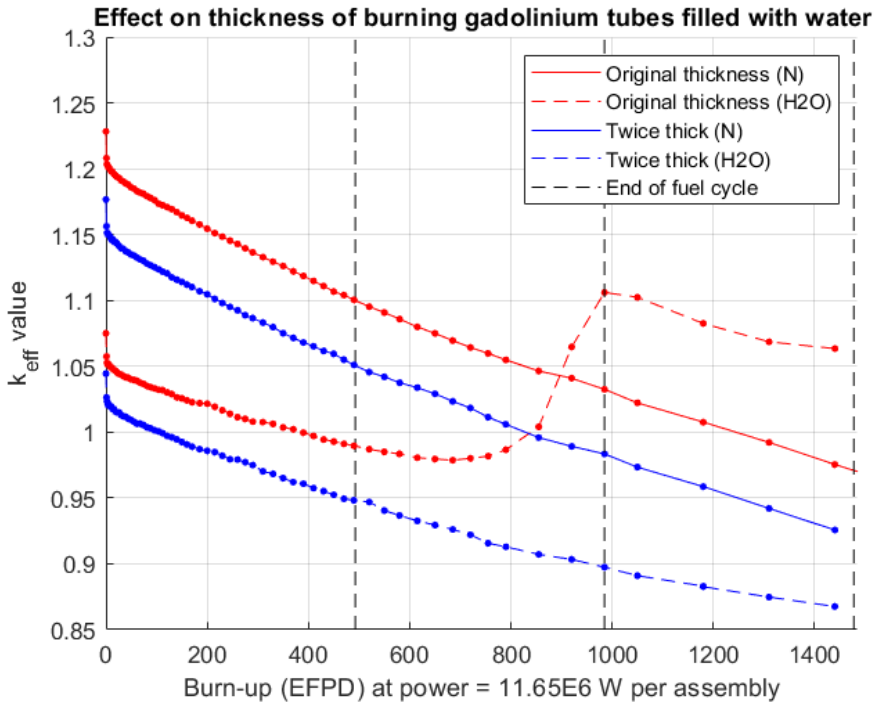


Fig. 2.6 Effect of tube thickness on burn-up
*10000 neutrons per generation, 500/200 active/inactive cycles, error* $4E-4$

### 2.3.2 Effect of Axial Discretisation

Figure 2.7 shows the progression of $k_{\text{eff}}$ with burn-up, with both the fuel and the control tubes burnt in 10 axially discrete zones. The figure shows that axial discretisation leads to a significantly longer cycle length and higher burn-up, a preferable trait. There are various reasons why this could be; one possible explanation is that the fuel in the centre of the pins, which experiences a higher flux, will have a more rapid capture cross-section reduction than the fuel near the periphery (due to its initially higher power), leading to a more uniform power distribution, which leads to increased fuel utilisation of the fuel in the periphery, and therefore a higher average burn-up. This leads to a fuel cycle length of 492.5 EFPD, or a total burn time of 1477.5 EFPD, corresponding to 52MWd/kg.

Now that the cycle length has been calculated, the material compositions at the corresponding states of burn-up can be taken to find the composition of each fuel batch at the start of the 3-batch fuel cycle (this is discussed further in Chapter 3). However, as PWRs are shut down between each fuel cycle for refuelling and potential maintenance, the fuel assemblies are able to 'cool-off' at near 0 power between the end of one cycle and the start of the next. This results in the decay of some short-lived fission products such as xenon-135. When modelling the starting composition of each fuel batch, it is therefore important to consider the material progression under zero power, as the reduction in neutron absorbers such as Xe-135 will have significant impact on the assembly-wise power distribution at the start of the next cycle. Hence Figure 2.7 also shows the cool-off of each batch at 0 power for 30 days. It can be seen that there is a significant increase in $k_{\text{eff}}$, which levels off after around 5 days.

## 2.4 Control Worth Characteristic

An important characteristic in nuclear reactors is the reduction in $k_{\text{eff}}$ for a given increase in control gain. This can help assess the reactor's behaviour in accidents, and help the design of a stable control system. Figure 2.8 shows the control curve for a fresh lattice, and at the end of one cycle before the tubes are replaced. The figure shows that the control curve is not linear, nor is it symmetrical around the 50% mark, unlike the S-curve of a conventional PWR control rod. One possible reason for this is that unlike a boron control rod, that is likely to absorb any neutrons that pass through it, due to their short mean free path, the S7G control tube relies on neutrons being moderated enough to then have a higher likelihood of being absorbed in the tube wall upon exiting the tube. Neutrons travelling predominantly in the x-y plane may not travel through enough water in the tube to significantly increase their chance of being captured in the wall upon exit, meaning that neutrons travelling with a significant velocity component in the z direction would make up most of the neutrons absorbed in the tube, as they can travel through a larger length of water. In this case, the proportion of the tube filled with water would be less significant than the height, as even if 10% of the tube is filled with water, this may not be a large enough length to cause significant moderation between tube entry and tube exit, leading to less

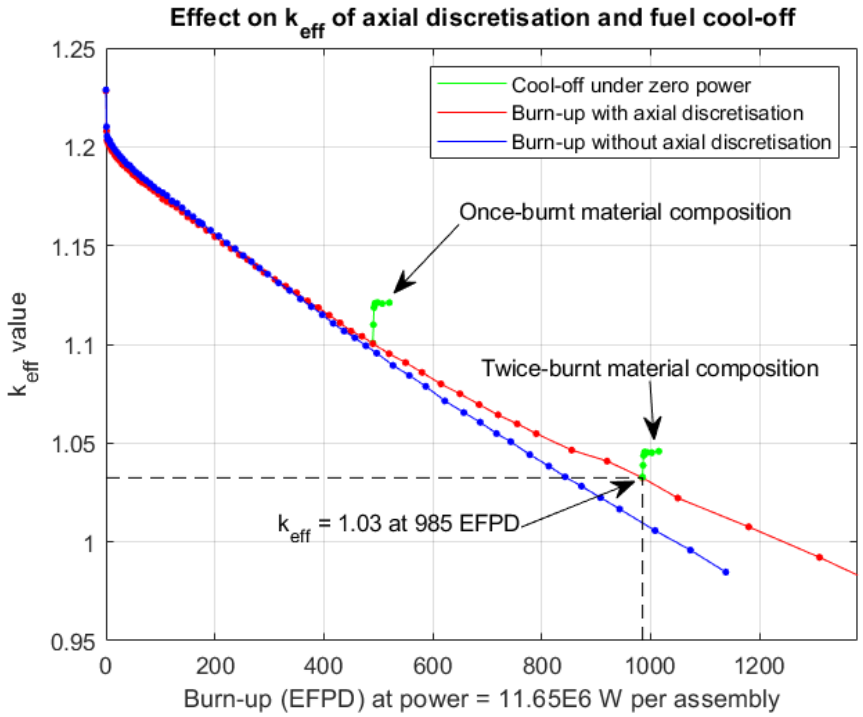


Fig. 2.7 Burn-up curve for axial discretisation and axial cool-off
*10000 neutrons per generation, 1000/200 active/inactive cycles, error* $2E-4$

than 10% of control being achieved, even when considering the effects of lower flux at the axial periphery. This could explain the skew of the control curve to the right, with significant control only being achieved from 50%+ water level. The lower flux at the top periphery is likely the cause of the levelling-off of control at 90% water level.

Figure 2.8 also shows the control curve for a lattice at the end of one fuel cycle, before the gadolinium tubes are replaced, for scenarios where the tube has been filled with water or with nitrogen. The figure shows that for both cases total $\Delta k_{\text{eff}}$ has decreased, as expected due to the burning up of the control tubes. $\Delta k_{\text{eff}}$ has decreased more in the water-filled tubed, due to the higher neutron absorption. The control curve is now more symmetric for the water-filled tube, with a higher initial gain, this is possibly due to the more axially uniform power distribution of the lattice, as the fuel in the centre has burnt-up faster than at the periphery. However, the tube burnt with nitrogen has not become more symmetric, suggesting that the tube state could have an effect on the axial burn-up of the fuel lattice.

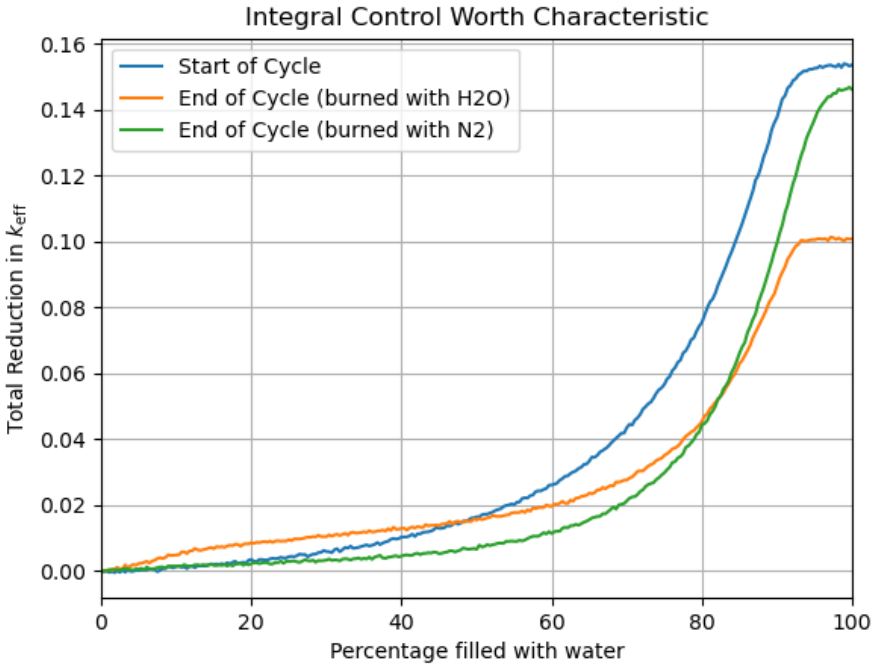


Fig. 2.8 Variation of $k_{\text{eff}}$ with control gain
*10000 neutrons per generation, 1000/150 active/inactive cycles, error* $3E-4$

# Chapter 3

# Design of a 3-Batch Core

## 3.1 Loading Pattern & PPF Considerations

In practice, the material composition of a fuel assembly after burn-up depends not only on the length of burn-up, but also its position in the core, as assemblies near the centre will burn up faster than those on the periphery. This makes designing a reshuffling scheme, to reorder the fuel assemblies between cycles, quite difficult, as there are 121 positions in the Rolls SMR (as compared to 193 in a typical, conventional PWR) and each position can inherit the fuel from any other, leading to a very large optimisation space.

For simplicity, it is assumed that each fuel assembly in the same batch, i.e. fresh fuel, once-burnt fuel and twice-burnt fuel, has identical material compositions, calculated from the single lattice burn-up curve as described in Chapter 2. Even with this assumption, there are several design choices to be made in the arrangement of the fuel in the core. Placing fresh fuel, which produces more neutrons, nearer the centre of the core reduces neutron leakage, thereby reducing the irradiation of the containment vessel, and associated physical stresses. However, fresh fuel at the centre increases the power at the centre, which risks causing power peaking problems, where the temperature of the central fuel pins may exceed their design limits quickly in the event of an accident. To guard against this, an assembly-wise Power Peaking Factor (PPF) is defined as the power of the highest power assembly in the core divided by the average assembly power of the core. A value for the maximum permissible assembly PPF is hard to find in nuclear regulation, as it is a function of the specific reactor design and other fixed limits, such as the maximum permissible fuel temperature (for melting), or the maximum heat flux (for the Departure from Nucleate Boiling Ratio). However, for many modern reactors, an assembly PPF limit of around 1.3 is typical [5].

There are two main methods used to decrease the PPF:

- Usage of Burnable Poisons: The use of burnable poisons involves adding neutron absorbing material to some of the fuel pins. As the poison is burnt up, the neutron absorbing isotopes are transmuted and their effect is reduced. In this way the reactivity is significantly lower

at the start of the cycle, and then converges on the behaviour of a fuel pin without poison later in the cycle. The use of burnable poison can displace some fissile fuel which leads to a small reactivity reduction even at the end of the cycle, which is undesirable. Adding burnable poisons to the locations with the highest power will reduce the local power density, reducing the PPF, and will also reduce the excess reactivity at the start of the fuel cycle which reduces the burden on the control tubes.

- Changing of fuel loading pattern: As discussed previously, placing fresh fuel towards the edges of the core can reduce the PPF. Providing the new layout does not have a significantly higher leakage, editing the loading pattern does not reduce $k_{\text{eff}}$ at the end of the cycle unlike the use of burnable poison. Changing the fuel loading pattern is also a simpler task than having to fabricate and manage many different fuel assembly configurations, which will be necessary if different burnable poisons are used throughout the fuel assemblies. Therefore the fuel loading pattern will be adjusted first, and burnable poisons will then be added afterwards if necessary.

Without burnable poisons, it is sufficient to calculate the PPF only at the start of the fuel cycle, as the high power regions will burn up faster than the lower power regions, reducing their power relative to the core average, therefore reducing the PPF. However, when burnable poisons are used, the highest $k_{\text{eff}}$ will not necessarily be at the start of the cycle, but may instead be later in the cycle, when the poison's effect has started to reduce. Therefore, it is important to consider how the PPF varies with burn-up as well. It is also important to consider how the use of control tubes effects the PPF, as unlike soluble boron which acts across the whole core, changing the water level in individual tubes will effect the power distribution around their location.

## 3.2 Loading Pattern Tests

Several standard fuel loading patterns were evaluated for use. Each pattern consisted of 121 assemblies, with 40 assemblies corresponding to each batch, with identical material compositions as described in Chapter 2. The 121st fuel assembly is the central assembly, which is managed separately from the three batches. To reduce power peaking at the centre, this central assembly often has lower enriched fuel which is burnt only once. For simplicity, it is modelled here as a twice-burnt fuel assembly. The core is surrounded by a 60cm radial reflector to reduce neutron leakage. The loading pattern diagrams shown in Figures 3.1 - 3.3 show a quarter of the core, with the central assembly in the bottom left of the figure. In the Serpent model, only an 1/8 of the core is specified, and then reflective boundary conditions are imposed due to the 8-way symmetry of the loading pattern, in this way the memory usage of the simulation is reduced. The axial and radial boundary conditions beyond the water reflectors are set to vacuum. Table 3.1 shows the start-of-cycle $k_{\text{eff}}$ and assembly-wise PPF for each loading pattern.

It is important to note that these PPF values do not accurately reflect the real PPF values during operation. This is due to several factors including:

- Uniform fuel temperature - higher power fuel pins will reach higher temperatures than the average pin, causing a decrease in reactivity due to the Doppler effect, and therefore will have a lower actual power than predicted in this simulation. Similarly, low power fuel assemblies would see a power increase due to operating at lower temperatures, therefore the overall power distribution would become more uniform, decreasing the PPF.
- Lack of control tube activation - the fuel loading patterns are all tested with no control gain. In reality, fresh assemblies which have a higher reactivity are likely to be filled with water, as the lack of soluble boron means many assemblies need to be filled with water at the start of the cycle to control the reactivity. When filled with water, the power of the assembly will change, changing the PPF values. This could reduce the PPF by reducing the power in peak assemblies, but also has the potential to increase the PPF, due to making the power distribution less uniform, as there could be large differences in power between nitrogen-filled and water-filled assemblies.

Despite these factors, finding the power distribution without control still gives a good indication of the underlying core power distribution, and can be useful to inform the design of burnable poisons and a control algorithm.

### 3.2.1 Checkerboard Pattern

Figure 3.1 shows a 121 assembly checkerboard pattern, adapted from the standard 193 assembly pattern [10]. The checkerboard pattern distributes fresh assemblies across the core, aiming to combine moderate neutron leakage with moderate power peaking, whilst obeying the constraint of having 40 fuel assemblies of each batch. The corresponding start-of-cycle PPF values can be seen in Figure 3.1b. It can be seen that the fresh assemblies closest to the core have a PPF value of 2.1, which is significantly higher than the approximate limit of 1.3.

### 3.2.2 Ring of Fire Pattern

Figure 3.2 shows the ring of fire loading pattern. This places the fresh fuel assemblies in a ring near the periphery of the core, with an outer ring of pre-burnt fuel at the outermost layer. By placing the fresh assemblies towards the periphery, this fuel pattern aims to reduce power peaking in the core centre, whilst also reducing neutron leakage, as there are no fresh assemblies at the outer layer of the core. The highest PPF value is 1.7, and Table 3.1 shows that the start-of-cycle $k_{\text{eff}}$ is slightly higher than that of the checkerboard pattern, due to the reduced neutron leakage, as no fresh fuel is directly exposed to the edge of the core.

### 3.2.3 Ultra-low power peaking

Figure 3.3 shows the ultra-low power peaking loading pattern. This aims to achieve the lowest PPF value possible by placing the most burnt fuel at the centre and the fresh fuel at the very edge.

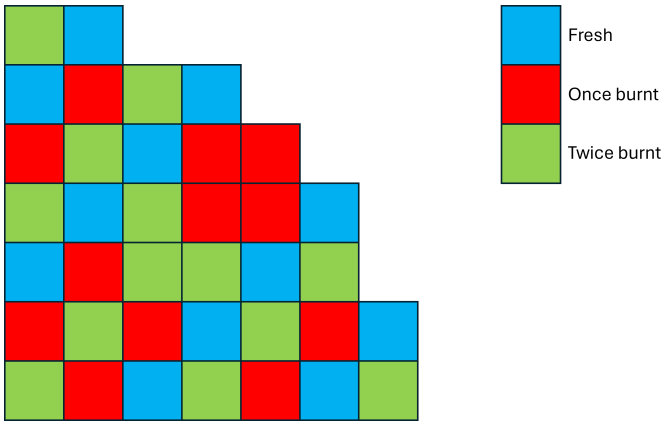


(a) Fuel loading pattern

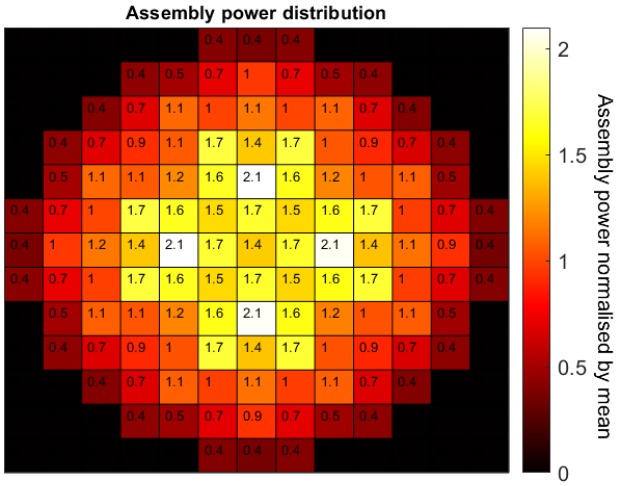


(b) Assembly-wise normalised core power distribution

Fig. 3.1 Checkerboard loading pattern characteristics

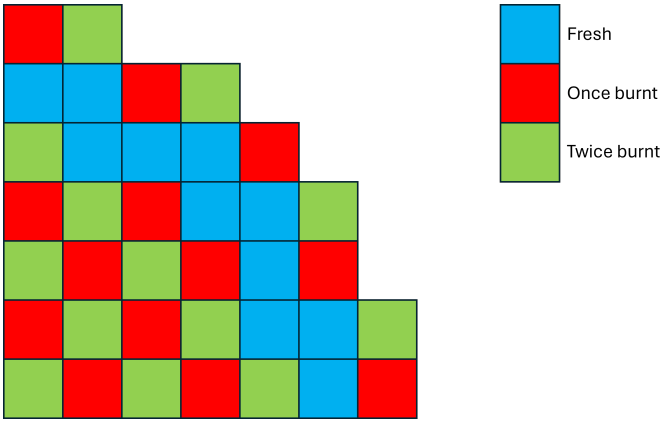


(a) Fuel loading pattern

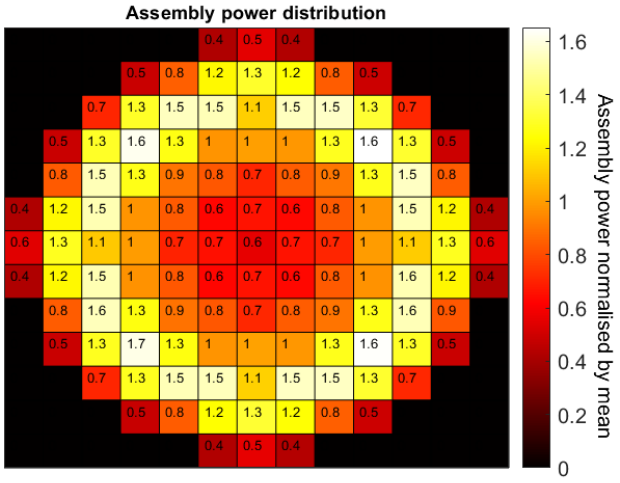


(b) Assembly-wise normalised core power distribution

Fig. 3.2 Ring of fire loading pattern characteristics

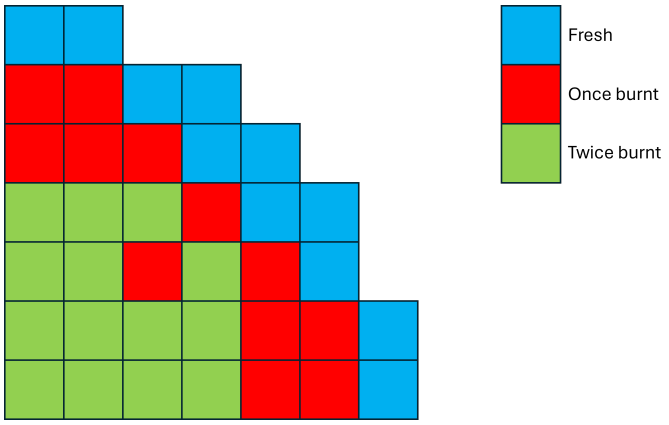


(a) Fuel loading pattern

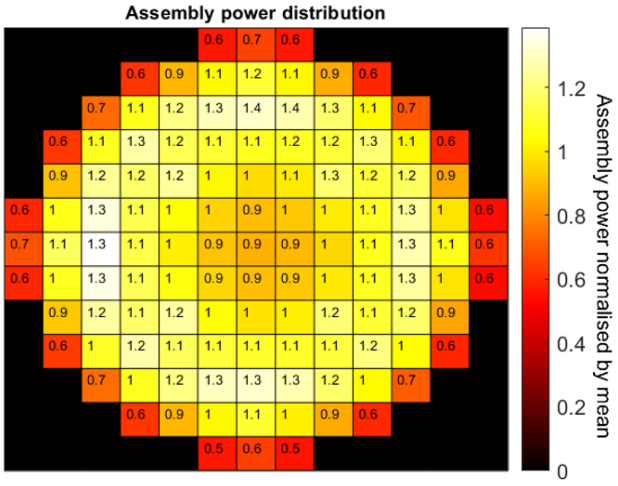


(b) Assembly-wise normalised core power distribution

Fig. 3.3 Ultra-low power peaking loading pattern characteristics

The maximum PPF is 1.4, which is only slightly above the 1.3 limit, and could well be within limits when considering the effect of a non-uniform fuel temperature distribution. However, the start-of-cycle $k_{\text{eff}}$ is much lower than that of the checkerboard pattern, as shown in Table 3.1.

### 3.2.4 Choice of Loading Pattern

Despite the low PPF of the ultra-low power peaking pattern, the low $k_{\text{eff}}$ suggests its burn-up performance will be much worse than the other two patterns, as it has half the excess reactivity. Half the excess reactivity suggests half an attainable burn-up when using the linear burn-up model, or significantly less when considering the fast drop in $k_{\text{eff}}$ due to Xe-135 production. Therefore, the loading pattern chosen for the S7G model was the ring of fire, as it had moderate power peaking, with the highest $k_{\text{eff}}$. The max PPF value of 1.7 suggests that burnable poisons will need to be designed.

| **Loading Pattern** | **PPF** | $k_{\text{eff}}$ |
|---|---|---|
| Checkerboard | 2.1 | 1.0919 |
| Ring of Fire | 1.7 | 1.1047 |
| Ultra-low Power Peaking | 1.4 | 1.0472 |

Table 3.1 Loading pattern characteristics

*100000 neutrons per generation, 800/200 active/inactive cycles, error* $7E-5$

## 3.3 Design of Burnable Poison

As the power peaking could not be handled through loading pattern design alone, the use of burnable poisons is required. Burnable poisons can be located in the fuel lattice, in place of regular fuel pins, or can be located at certain points in the core where flux is expected to be highest. As in the previous work [6], this project will incorporate burnable poison in the form of an annulus around standard fuel. The poison will displace some of the fuel in poisoned pins, in order to keep the outer diameter the same.

There are several characteristics that good burnable poison design should seek [4]:

- Minimal reactivity penalty when fully burned-up
- Minimal effect on thermal conductivity in fuel
- Burn-up curve to match fuel burn-up
- Chemical/corrosive compatibility with fuel/fission products

Gadolinium based poisons are commonly used, and were chosen for this model as a $Gd_2O_3$ - $UO_2$ mix, due to the known chemical compatibility. The mixture ratio was fixed at 7% $Gd_2O_3$, as 7% is the usual limit in commercial fuels to avoid stronger effects on the thermal conductivity [2]. Several different poison loading schemes were designed for the fresh fuel assemblies, depending on their location in the core and the flux experienced. The number of poisoned pins in each fresh fuel assembly is shown in Figure 3.5. Figure 3.6 shows the loading scheme for the highest power fresh assembly, with 32 poisoned pins shown in green. The dimensions for the poisoned layer are displayed in Table 3.2, with the geometry displayed in Figure 3.7.

Figure 3.4 shows the burn-up curve for the most poisoned lattice, when modelled as infinite in the x-y plane, and 2.8m in height. The figure shows that there is minimal reactivity penalty when the poison is fully burned-up, with $k_{\text{eff}}$ of the poisoned and non-poisoned lattice being approximately the same by the end of one fuel cycle. This supports the approximation that the once-burnt and twice-burnt batches can be modelled as homogeneous groups, despite having different amounts of poison when fresh. One criticism of the design is that the initial drop in $k_{\text{eff}}$ is too large, reducing $k_{\text{eff}}$ to below the value at the end of one cycle, resulting in a non-flat burn-up curve. This suggests that the lattice contains too many poisoned pins (due to the initial drop), with too low a gadolinium content in each poisoned pin (due to the non-flat profile). A

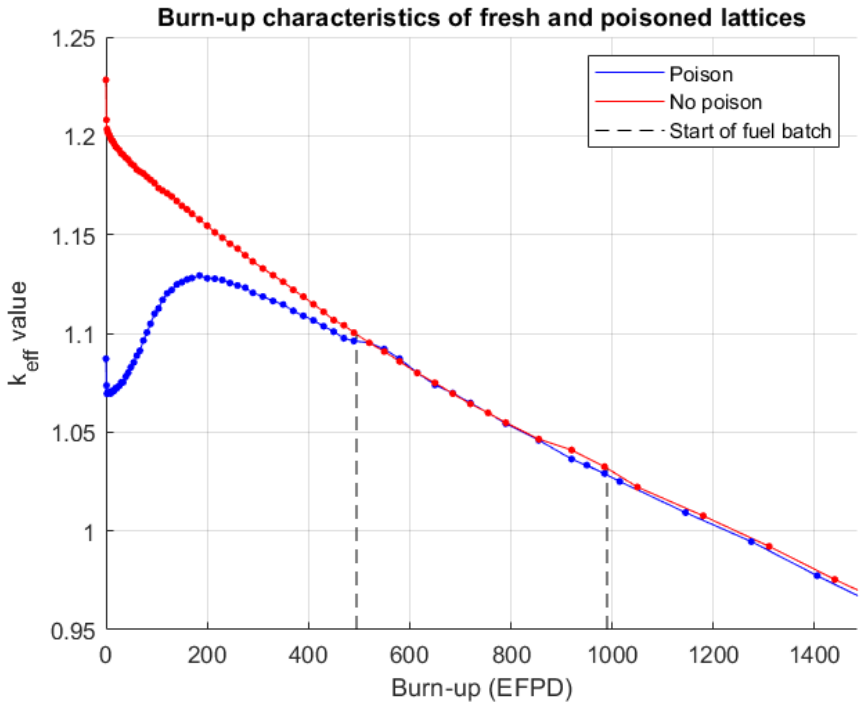


Fig. 3.4 Effect of burnable poison on lattice burn-up
*10000 neutrons per generation, 600/150 active/inactive cycles, error* $3E-4$

more sophisticated poisoning regime could use different thicknesses of poison in each fresh assembly, depending on the experienced flux, and could fine tune the number of poisoned pins to ensure a flat burn-up profile.

## 3.4 3-Batch Core Performance

### 3.4.1 Power Peaking with Poison

Figure 3.8 shows the start-of-cycle PPF values for the final fuel and poison loading pattern. During testing there were power peaking problems in the centre, therefore the central assembly was replaced with a 3% enriched fuel assembly, which will only be burnt for one cycle. The highest PPF is now 1.36, which is likely a statistical overestimate, as the 3 assemblies in symmetrical locations have a PPF of 1.3 or below, and the reported error in the PPF values is 3.5%. It is also likely to be an overestimate due to the non-uniform fuel temperature as discussed previously.

### 3.4.2 Whole Core Burn-Up

Figure 3.9 shows how the $k_{\text{eff}}$ of the whole core varies over the course of the fuel cycle. A cycle length of 455 days is suggested before the core becomes unable to sustain the chain reaction. As the input geometry for the once and twice-burnt batches assumed a cycle length of 492 days, it is clear that the whole core behaviour is not perfectly captured by the linear and partial reactivity

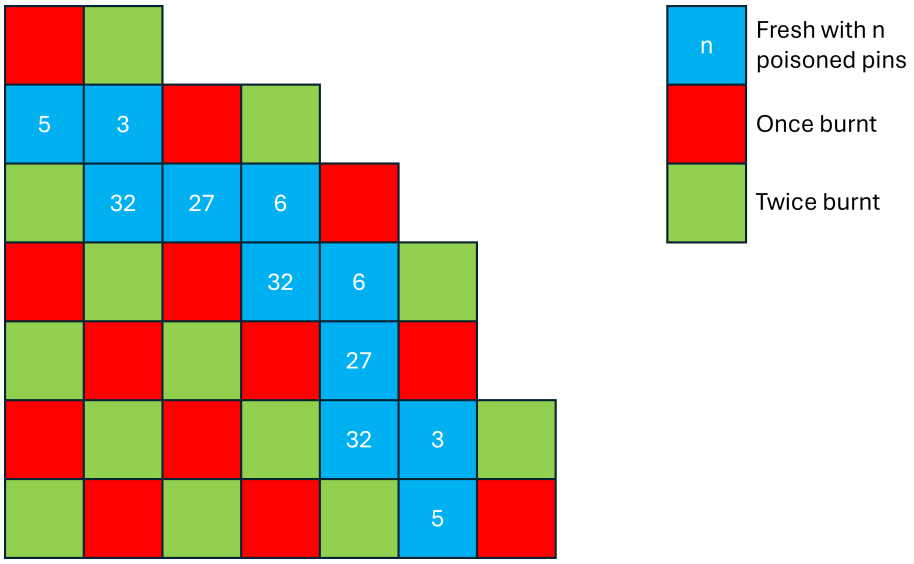


Fig. 3.5 Poison core loading pattern

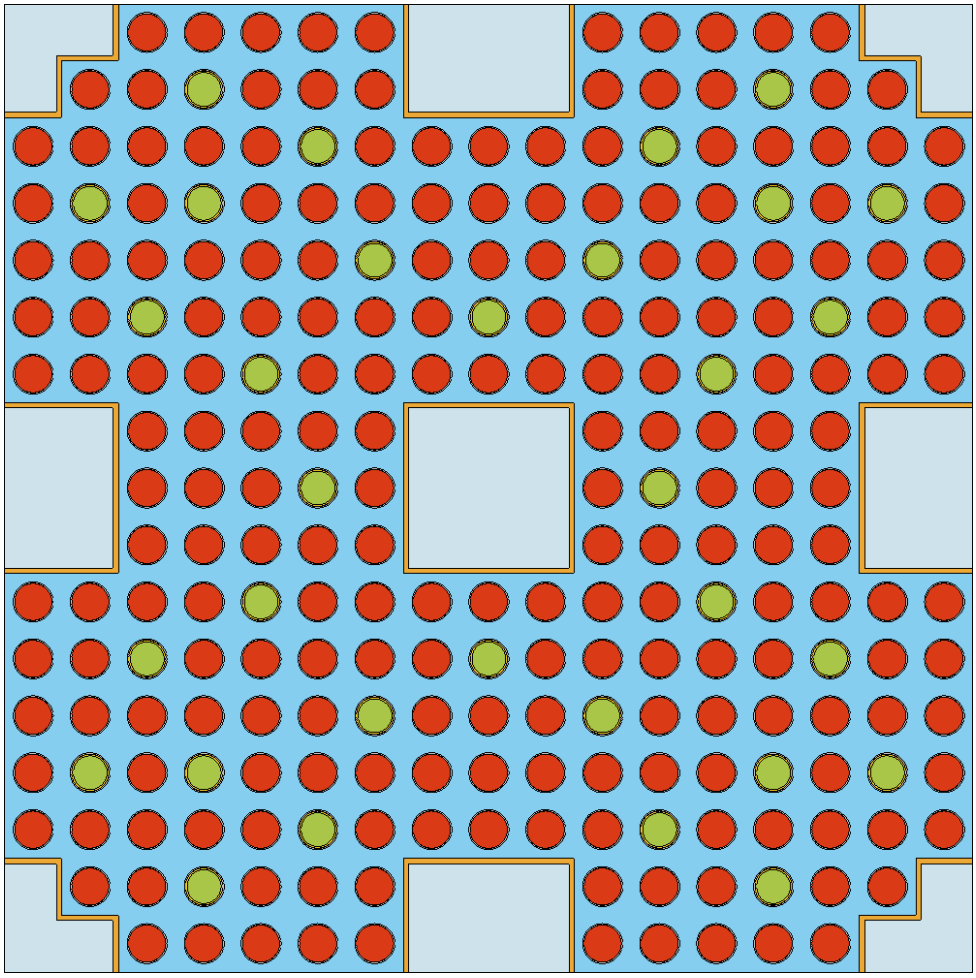

Fig. 3.6 Poison loading design with 32 poisoned pins, shown in green

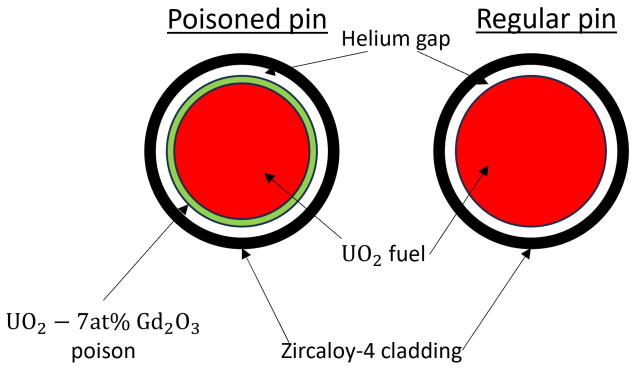


Fig. 3.7 Poisoned fuel pin geometry

| Part | Size (cm) |
|---|---|
| Outer radius of $UO_2$ | 0.3754 |
| Outer radius of $UO_2$-$Gd_2O_3$ | 0.4096 |
| Outer radius of helium gap | 0.4138 |
| Outer radius of Zircaloy-4 cladding | 0.4423 |

Table 3.2 Poisoned fuel pin dimensions

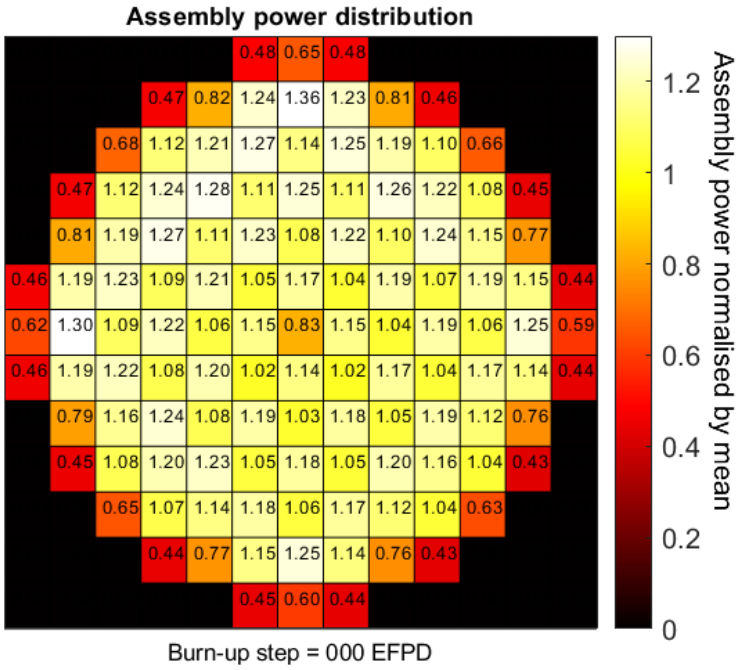


Fig. 3.8 Start-of-cycle assembly-wise normalised PPF for final core geometry
*100000 neutrons per generation, 800/200 active/inactive cycles, error 3.5%*

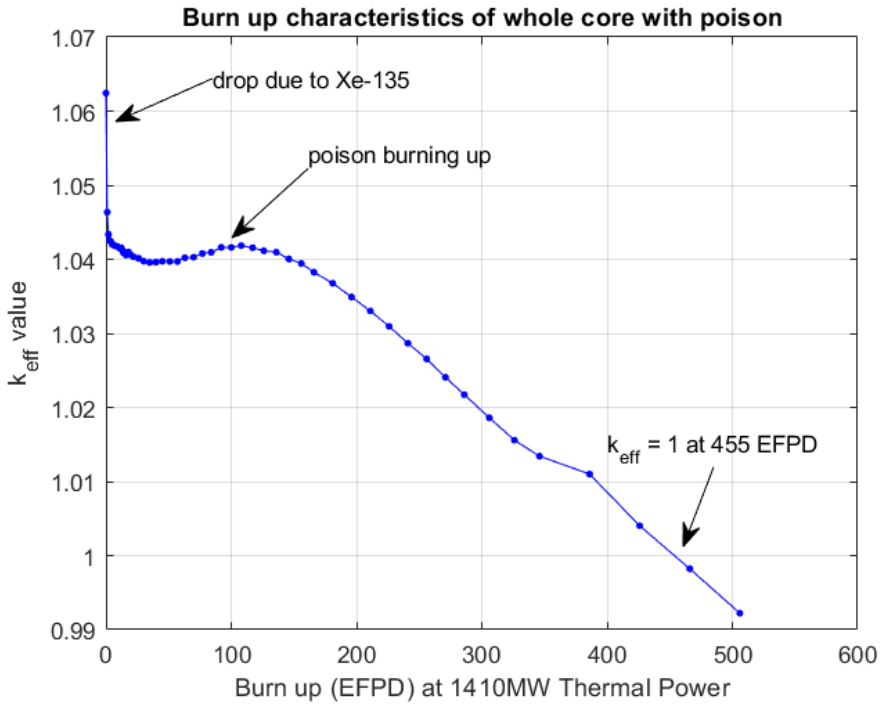


Fig. 3.9 Variation of $k_{\text{eff}}$ with whole core burn-up
*100000 neutrons per generation, 1000/100 active/inactive cycles, error* $7E-5$

models. Therefore, the simulation could be made more accurate by its repetition with fuel lattices burnt with a cycle length of 455 days. This modification would then suggest a slightly different cycle length for the whole core. An iterative process would be necessary to converge on the actual cycle length, which will not be done at this point due to the computational expense of a whole core burn-up simulation.

### 3.4.3 Key Design Points

Table 3.3 shows the $k_{\text{eff}}$ value of the 3D reactor at the start and end of the fuel cycle. The density of the light water moderator was adjusted with temperature, but the thermal expansion of fuel was not modelled. The $k_{\text{eff}}$ is considered under three operating points:

- Hot full power: the reactor is assumed to be at rated power, at its operating temperature. With all control methods removed, it is important that $k_{\text{eff}} > 1$ so that the chain reaction can be sustained. During operation, the use of control methods would fix $k_{\text{eff}} = 1$ to keep constant power.
- Hot shutdown: the reactor is at its operating temperature, and has just had all the control tubes fully filled in order to stop the fission chain reaction, transitioning from full rated power to zero electrical power (There will be residual fission product decays which correspond to a non-zero core power). It is important that $k_{\text{eff}} < 1$ so that the chain reaction can be halted. When fission is halted, the temperature of the fuel will drop almost

| **Run** | Cold zero power | Hot shutdown | Hot full power |
|---|---|---|---|
| **Fuel T(K)** | 300 | 630 | 900 |
| **Cladding T(K)** | 300 | 630 | 630 |
| **Water T(K)** | 300 | 570 | 570 |
| **Control Tube T(K)** | 300 | 600 | 600 |
| **Water level (%)** | 100 | 100 | 0 |
| $k_{\text{eff}}$ **Start of Cycle** | 0.9887 | 0.9448 | 1.0624 |
| $k_{\text{eff}}$ **End of Cycle** | 0.9277 | 0.8800 | 1 (assumed) |
| **Error** | 1.5E-4 | 1.5E-4 | 1.3E-4 |

Table 3.3 : $k_{\text{eff}}$ values for the whole core
*100000 neutrons per generation, 800/200 active/inactive cycles*

instantaneously, leading to a positive reactivity insertion due to the Doppler Coefficient, but the temperature of the coolant will initially remain the same as during hot full power.

- Cold zero power: the reactor is shut down at room temperature. Nuclear reactors typically have a negative moderator temperature reactivity coefficient to ensure negative feedback at full power, meaning an increase in temperature leads to a decrease in power, lowering the temperature. This is achieved as at lower temperatures the water moderator is denser, increasing its moderating capability, increasing the proportion of thermal neutrons, thereby increasing the likelihood of a neutron causing a fission event. A counter effect of a high moderator density is that the absorption rate of neutrons in the moderator is higher, but this effect is typically smaller than the first. This means that when the reactor is shut down and the temperature is at its lowest there is an increase in reactivity. Therefore, a key design point is to ensure that $k_{\text{eff}} < 1$ at room temperature.

The table shows that $k_{\text{eff}}$ is within limits for all the key design points. As the fuel is burnt up, the core $k_{\text{eff}}$ will decrease, meaning the cold zero power and hot shutdown cases should remain within limits for the length of the fuel cycle, providing there is not a significant change in the moderator temperature coefficient with burn-up, which we have validated by also calculating the values for the end of cycle.

### 3.4.4 Tube Energy Deposition

Most fission energy is deposited directly in the fuel, and then needs to be conducted through the fuel, gap and cladding in order for the heat flux to reach the coolant, causing a temperature gradient between the centre of the fuel and the coolant. However, some energy is released from the fission process as photons, which can travel through the fuel to the light water coolant before depositing their energy. Energy can also be deposited directly in the coolant due to neutron transport, where energy is transferred during collisions. In a conventional PWR, this direct energy deposition is not usually a critical cause for concern, as depositing energy directly in the coolant reduces the temperature gradient necessary for heat transfer, and therefore reduces

the maximum fuel temperature. However, in the S7G reactor, not all the light water serves as the coolant, due to the water present in the control tubes. If the water in the control tubes is not cooled or circulated out of the core adequately quickly, this energy deposition could cause boiling of the control tube water. Whilst conventional PWRs typically have a negative void coefficient for the coolant, this is not true for the control water in the S7G, and so this boiling process could cause a positive feedback loop, leading to reactor instability.

The fraction of energy deposited in the control tubes was therefore calculated by using a total energy deposition detector, which records energy deposition due to fission, neutron heating, and analog photon heating. For combined neutron-photon transport calculations, Serpent requires extra ACE-library data than is included in JEFF31, and so the cross-section data for this simulation alone was changed to ENDFB7. The KERMA data files (the coefficients needed for photon transport) distributed on the Serpent Wiki, do not include data for every nuclide, and this is one of the reasons why the combined neutron-photon transport simulation mode is not recommended to be combined with burn-up simulations [13]. Indeed, when the whole core 3D mock-up was simulated in this mode, Serpent crashed due to mismatches between the standard and KERMA ACE-libraries, for several nuclides in the material composition of the once and twice-burnt batches. Therefore, the simulation was conducted on a fresh infinite lattice at 0 burn-up, filled with water. The detector was split into 17 bins in the $x$ and $y$ directions, with each bin centered around one pin position, and with the bin side length corresponding to the lattice pitch.

Figure 3.10 shows the energy deposition at each position in the lattice. The figure is plotted in a log 10 scale, to ensure that the values for the control tube deposition are visible. The deposition per lattice position is just under 2 orders of magnitude lower in the control tubes than it is in the fuel pins and surrounding coolant. When summed over all pins, the total energy deposition across the lattice was confirmed as 11.65 MW, as expected due to the set power, of which 42.31 kW, or 0.36% , was deposited in the control tube water and walls. This corresponds to a significant heating power, and taking the enthalpy of phase transformation as $h_{fg} = 1000.5$ kJ/kg (the value for 150 bar), this is enough to boil the 15.9kg of water in the tubes every 6.3 minutes. Therefore, a minimum pumping rate of 2.52kg/min would be needed for an average-power assembly, with a higher rate for assemblies with higher powers. When filled with nitrogen, the energy deposition was negligible in the tubes, being 2 orders of magnitude smaller than the water-filled deposition.

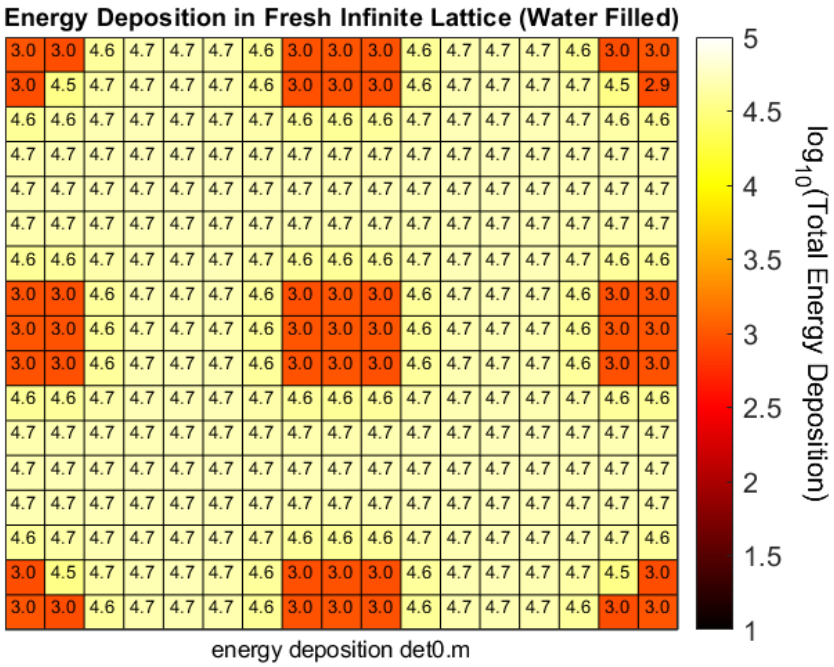


Fig. 3.10 Energy deposition distribution in a fresh lattice, shown on a log scale
*10000 neutrons per generation, 1000/200 active/inactive cycles*

# Chapter 4

# Control Algorithm Design

In the previous chapters, a model has been constructed that has shown feasible operating points of the S7G reactor at the start and end of the fuel cycles. However, as the major difference between the S7G and a conventional PWR is the control system, the real substance of this project is to investigate whether the control tubes can exercise effective control over the core. For this to be the case, $k_{\text{eff}}$ must be kept equal to 1, ideally with the PPF obeying the limit of 1.3.

## 4.1 Binary vs Variable Tubes

As the control gain curve is strictly increasing, the simplest method of controlling $k_{\text{eff}}$ would be to gradually lower the water level in all tubes over the length of the cycle. However, this would cause large axial asymmetries in power and therefore burn-up, and would lead to under-utilisation of the fuel at the bottom of the reactor, which would be the last section to be emptied of water. This under-utilisation would lead to a lower average discharge burn-up, and therefore fuel cycle length, leading to negative economic consequences. Therefore, it is likely preferable to operate tubes in a binary manner, wherein they are either full or empty, in order to reduce axial asymmetries. Operating tubes as either full or empty may well simplify the pumping equipment necessary for the tubes, and reduce the burden on sensors and control systems needed to keep the water level at a specific value. However, it is obvious that a discrete tube activation system cannot fine tune $k_{\text{eff}} = 1$ at all points in burn-up, due to its value being continuous in nature. Therefore, whilst the bulk of tubes should operate in a binary manner, a minimal number, to be determined, will need to be operated in a continuous manner.

### 4.1.1 Pumping Mechanism & Safety Considerations

As discussed in Section 3.4.4, even completely full control tubes need a pumping regime in order to circulate the water and avoid boiling due to photon energy deposition. In addition, some safety mechanism needs to be added, so that in a loss of coolant (LOCA) or loss of power accident, the control tubes are flooded in order to shut down the reactor. The original S7G design had a reservoir of water above the tubes constantly flooding them with water, and a pump that pumped

the water out at the same rate in order to keep the level constant [14]. This had the advantage of ensuring the tubes were flooded in the event of a power failure that disabled the pumps. Whilst the modelling of the pump is beyond the capability of Serpent, it is recommended that a similar system is used, with a flow rate set by the photon energy deposition, plus appropriate safety margin.

In the event of a LOCA, it is less clear how the reactor would behave. A whole core loss of coolant would remove the moderator as well as the control water, creating problems with decay heat removal, but also ensuring that the reactor would not become critical after the coolant has all drained from the core; however, the transient behaviour during blowdown is less clear. As the flow diameter in the control tubes is 2-3 times the scale of the lattice pitch, the possibility of the control tubes draining faster than the coolant, for example due to some debris from the reactor pressure vessel (RPV) rupture stuck in the fuel lattice, cannot be totally neglected, and this could pose a real danger of criticality during the accident. However, if the tubes are sealed at the bottom, and are only filled/pumped empty from the top, this should reduce the likelihood of their draining during an RPV rupture.

### 4.1.2 Lattice-wise Tube Activation

As shown in Figure 1.1, 8 of the 9 tubes which feature in the lattice lie on the lattice boundary, meaning they are only sealed due to the tessellation of numerous assemblies in the core. Having two adjacent assemblies with different water levels in the control tubes is therefore non-physical, as the water would settle in the tube to give the average water level of all intersecting assemblies. A practical pumping mechanism would be to control each tube or bank of tubes as one unit, ignoring the fact that they intersect assembly boundaries. However, redefining the geometry in Serpent to allow this would be quite difficult, and may increase the memory consumption of the model due to increasing the number of cells and geometry definitions. Therefore, the existing model will be adapted by adding a 2mm Zircaloy-4 divider in the tubes at lattice boundaries, allowing the water level to be split in different sections of the tube. This also means that the tubes in the assemblies at the edge of the core will be sealed.

Table 4.1 shows the effect on $k_{\text{eff}}$ of adding the Zircaloy divider, and with a $k_{\text{eff}}$ reduction of less than 0.01 across the reactor, it is assumed that it has minimal negative impact. Therefore, in the following sections, an assembly's 'tube' refers to the set of 9 tubes intersecting with that assembly, rather than any one individual tube, unless stated otherwise. If the geometry were redefined so that each of the 9 tubes in a lattice could be controlled individually, easier reactivity control could be facilitated, along with a more uniform radial power distribution, due to decreasing the minimal $k_{\text{eff}}$ increment available to be changed, and by spreading out the changes across more assemblies, allowing finer control of the PPF.

| Tube State | No Zircaloy $k_{\text{eff}}$ | Zircaloy $k_{\text{eff}}$ |
|---|---|---|
| Water | 1.0813 | 1.0749 |
| Nitrogen | 1.2368 | 1.2286 |

Table 4.1 Effect of adding Zircaloy tube dividers on whole core model at start-of-cycle. *10000 neutrons per generation, 1000/100 active/inactive cycles, error 2E-4*

## 4.2 Algorithm Design

Whilst Serpent 2 has the ability to perform critical boron concentration searches [7], it lacks the ability to perform critical control rod position searches, which may have been generalisable to the control tube water level problem via the appropriate definition of geometry. Therefore, in order to find the level of variable control tubes needed to keep $k_{\text{eff}} = 1$, an iterative process would be needed at every point in burn-up, both to find the states of the binary control tubes, and then to fine tune the variable level, with a separate Serpent simulation executed at each burn-up step.

To facilitate the execution of various simulations in series with the simulation input dependent on the results of the previous one, a Python script was made to automate the simulation execution. While using a Python script speeds up the execution of a whole burn-up control series of simulations, it also creates problems when used in conjugation with a SLURM queue management system, which was needed as the size of the whole core model was such that it could only be executed on the University HPC centre. Whilst individual Serpent simulations could be executed as MPI jobs on the data centre, when launched from a Python script, they lacked the necessary permissions to be distributed over several HPC nodes. This meant that when using a Python script to conduct the burn-up simulation, simulations could only be executed with OMP parallelisation, leading to longer run times. Combined with the job run-time limits on the HPC, and the need to use paid HPC resources effectively, various assumptions were made to reduce the complexity of the control logic.

Figure 4.1 shows the algorithm design for designing a control tube activation scheme to manage burn-up, with each box of the flow chart representing a key function in the program. At each stage of burn-up, an appropriate control tube state is found that can satisfy the specified reactivity and PPF limits, and the core is then depleted with the control tubes in said states, accounting for non-uniform burn-up due to flux variations caused by the control tube states. As mentioned earlier, accuracy must be balanced against resource use, and so for each function there are various ways of implementing the algorithm.

### 4.2.1 Can $k_{\text{eff}}$ be controlled to 1?

During operation, $k_{\text{eff}}$ must be controlled to 1 to ensure safe steady-state operation of the reactor, which necessitates finding the continuous water level in the variable tubes necessary to fine tune the reactivity. However, if it can be shown that for a fixed binary control tube state that $k_{\text{eff}} > 1$

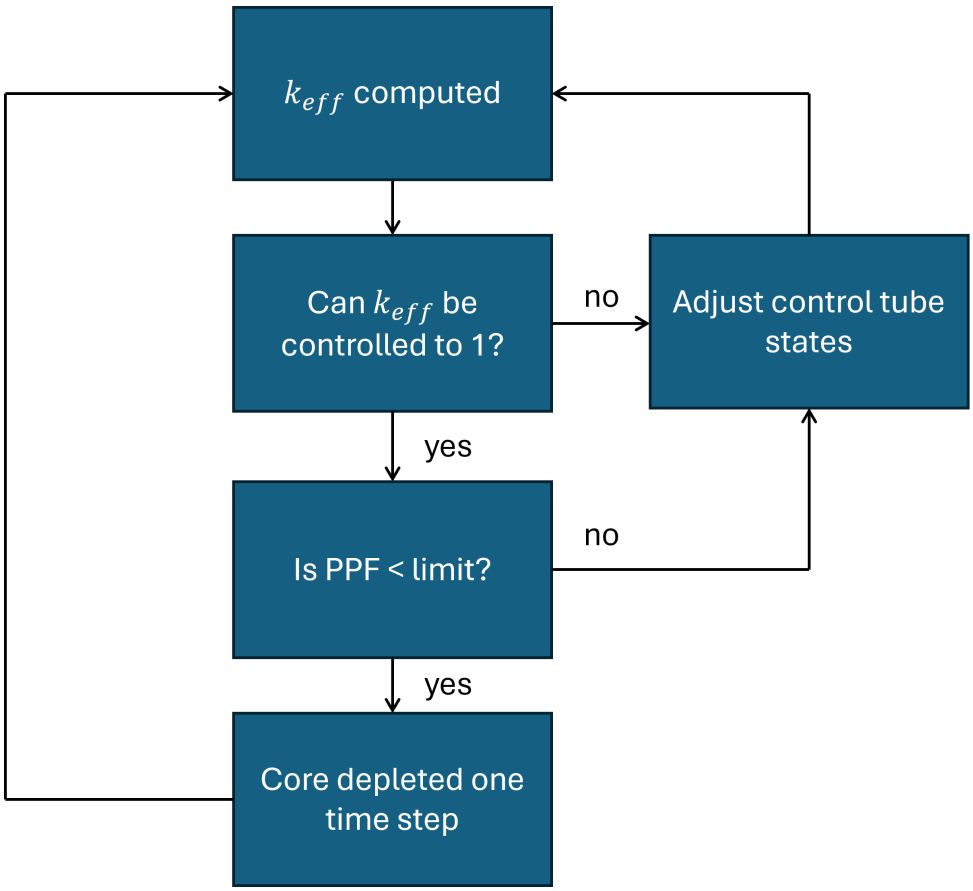


Fig. 4.1 Reactivity control algorithm

with the variable tubes filled with 100% nitrogen, and $k_{\text{eff}} < 1$ with the variable tubes filled with water, we can assume that fine-tuned control is possible without finding the exact water level required, thereby saving many computing resources by avoiding extra iterative simulations. Moreover, if the control gain of all the variable tubes can be approximated as $\Delta k_{\text{var}}$, then the reactor can be assumed stable if $1 > k_{\text{eff}} > 1 - \Delta k_{\text{var}}$ with the variable tubes filled with water.

Choosing what value to approximate $\Delta k_{\text{var}}$ as depends on both the number of variable tubes, and their individual control gain. With only 1/8 of the core being modelled in Serpent, control tubes could either be controlled in banks of 8 (most positions in the wedge), or in banks of 4 if sitting along the lines of symmetry (along the x-y axis or diagonals). Whilst it may be possible to fine tune reactivity using only 4 variable tubes and 117 binary tubes, it was decided to designate 8 tubes as variable, in order to increase $\Delta k_{\text{var}}$ and the number of control tube states meeting the operating requirements. The position of the 8 variable tubes can be seen in Figure 4.5. This would also increase redundancy in a physical system. The tubes chosen to act as variable tubes were the fresh assemblies on the x-y axis and diagonals, as shown in Figure 4.5, as fresh assemblies were thought likely to have a higher $k_{\text{eff}}$ due to their increased reactivity. The initial $\Delta k_{\text{eff}}$ of a fresh lattice is approximately 0.2, therefore the effect on the core was approximated as $0.2 \times \frac{8}{121} = 0.0132$. $\Delta k_{\text{var}}$ was set as 0.01, to allow for shadowing and effects of burn-up, leading to $1 > k_{\text{eff}} > 0.99$ being taken as the acceptable operating range. The accuracy of this approximation can be validated after allowing the algorithm to find suitable control tube states, by rerunning each burn-up step with the variable tubes empty, and validating that $k_{\text{eff}} > 1$.

### 4.2.2 Is PPF < limit?

Designing a control tube activation regime is of minimal utility if it produces unsatisfactory PPF values. However, with the limitations on assembly-wise tube activation discussed in section 4.1.2, and the uniform temperature distribution meaning that the Doppler effect cannot make the power distribution naturally more uniform, it is reasonable to expect that the PPF values obtained in the simulations are larger than those that would actually be obtainable in a real S7G reactor. When the algorithm was run with a PPF limit of 1.3, it often got stuck iterating through different combinations of control tubes at the same point in burn-up, leading to SLURM job time-out before a solution could be found. Whilst it may be possible to obtain PPF < 1.3 with the current model given enough computing resources, it was decided to impose a higher limit of 1.5, to allow for the overestimation and to conserve resources.

Whilst temperature variations could not be modelled during a whole burn-up simulation without unduly affecting performance, due to creating many more material and geometry definitions for each different temperature assembly, it was possible to estimate the effect on PPF of temperature in a standard criticality simulation. Figure 4.2a shows the core modelled at the start of burn-up, the control tubes have been selected in such a way as to deliberately induce a maximum PPF of above 1.5. The variation of fuel and cladding temperature was then assumed

linear with assembly power. In reality, whilst the temperature difference between the coolant and cladding, and the cladding and centre of the fuel pin, will scale linearly with power, assuming no temperature dependence of thermal conductivity or convective heat transfer, the temperature within the fuel will not have a linear variation. In addition, the magnitude of the Doppler effect will depend most strongly on the temperature at the edge of the fuel pin, as most U-238 absorption occurs here, due to the neutron self-shielding effect. The outer radius of the pin also contains more material, therefore the use of a volume-weighted average temperature can be useful when choosing a temperature to evaluate the magnitude of the Doppler effect. However, as a first-order simple approximation, these effects were not considered, and the temperature of each fuel pin was calculated via:

$$T_{fuel} = \Delta T_0 \times PPF + T_{coolant}$$

where $\Delta T_0$ is the original temperature difference between the average fuel temperature and the average coolant temperature, i.e. $900 - 570 = 330$K. Figure 4.2b shows the normalised assembly PPF values when considering the temperature variation. It is clear that the resulting reduction in PPF does not reduce the max PPF to below 1.3, with the two highest PPFs of 1.52 and 1.49 only being reduced to 1.46 and 1.43. However, what is clear is that the max PPF has decreased, and with all the fuel temperature modelling assumptions discussed above, combined with other assumptions such as the coolant temperature not varying axially, it is still of interest to use a higher limit of 1.5, if it allows the algorithm to converge using markedly less computing resources.

### 4.2.3 Adjusting Control Tube States

The control tube states are varied during the following scenarios:

- $k_{\text{eff}}$ is too low -> one control tube (per 1/8 core) is emptied
- $k_{\text{eff}}$ is too high -> one control tube (per 1/8 core) is filled
- PPF is too high -> one tube emptied and one tube filled

Whilst using soluble boron to provide whole core control induces negative reactivity across all lattices, using control tubes provides the potential for large peaks and troughs in the power distribution. Therefore the effect on PPF must be considered when choosing what tube to empty/fill. When changing the control tube states, the program reads the results of the assembly power detector of the previous simulation, and empties the tube with the lowest power, and/or filled the tube with the highest power, in order to make the power distribution more uniform.

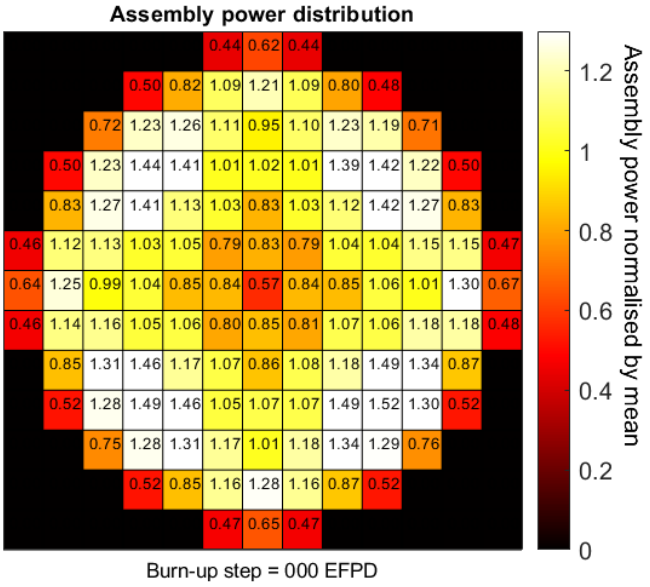


(a) Normalised assembly PPF with uniform assembly temperatures

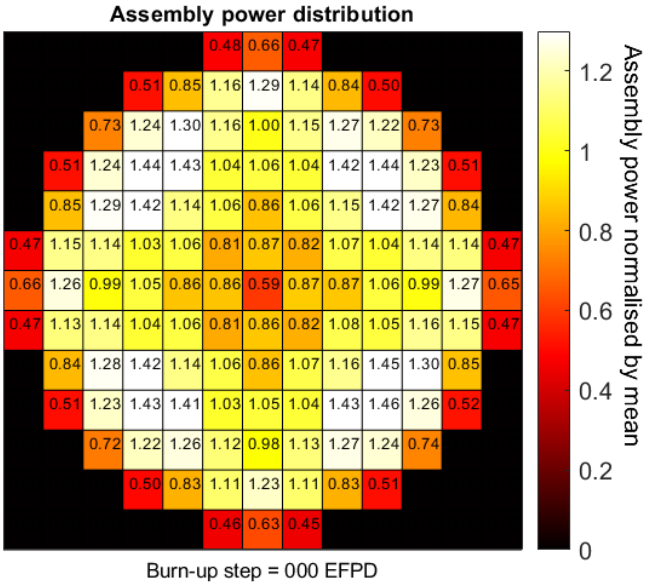


(b) Normalised assembly PPF with assembly temperature calculated from powers in 4.2a

Fig. 4.2 Effect on PPF of modelling temperature variation

## 4.3 Algorithm Performance

### 4.3.1 Reactivity Control

Figure 4.3a shows the variation of $k_{\text{eff}}$ with burn-up during the control sequence. The figure shows, that at each point in burn-up, the $1 > k_{\text{eff}} > 0.99$ condition can be achieved whilst keeping the variable tubes full and varying the states of the remaining tubes. It also shows, that when the simulation is rerun with the binary tubes in the same states and the variable tubes empty, that $k_{\text{eff}} > 1$ until 250 EFPD, at which point the decreasing $\Delta k_{\text{eff}}$ of the tubes, due to burning up, fails to keep the core critical, indicating that the $1 > k_{\text{eff}} > 0.99$ condition is not sufficient to maintain steady-state control for the whole of the fuel cycle. At around 40 EFPD, it can be seen on the figure where the control algorithm has emptied a tube for only one burn-up step, in an attempt to control the max PPF, whilst obeying the constraints on $k_{\text{eff}}$. The algorithm was not able to control the PPF < 1.5 at this point, but it moved on after 4 iterations in order to conserve resources.

The burn-up simulation was therefore rerun with a variable lower $k_{\text{eff}}$ limit, starting at $1 > k_{\text{eff}} > 0.99$ and increasing to $1 > k_{\text{eff}} > 0.993$ at 245 EFPD. The new variation of $k_{\text{eff}}$ with burn-up is shown in Figure 4.3b. The step at 40 EFPD was also run with more iterations in order to manage the PPF value, leading to it staying below the 1.5 limit, and giving a smoother $k_{\text{eff}}$ curve. The figure shows that with this variable limit, the reactor can be kept critical at each point in burn-up. At 390 EFPD, all tubes have been emptied, giving a final fuel cycle length of around 400 EFPD, allowing time for the excess reactivity in the system at 390 EFPD to decrease.

### 4.3.2 Control Tube Utilisation Statistics

Figure 4.4b shows how often each control tube bank (corresponding to one assembly in the 1/8 model, and every other assembly constrained to behave the same way by symmetry) changes states, i.e. is either filled or emptied. The control bank labelling scheme is shown in Figure 4.4a. The figure shows that the twice-burnt assemblies are never used by the control algorithm, likely because filling them would increase the maximum PPF by decreasing the power of the lowest power assemblies, necessitating a rise in power from the other assemblies. Therefore, the twice-burnt assemblies effectively act as a large shutdown bank for the reactor, and also provide redundancy in case of tube failure in the other assemblies.

This also has ramifications for the thickness of gadolinium needed in the control tubes, as if during the 3rd fuel cycle the assembly is not burnt when filled with water, which degrades the gadolinium much quicker than when filled with nitrogen, the wall thickness may not need to be designed to withstand a full 3 fuel cycles; it may only need to last 2 cycles, plus a margin to allow effective shutdown control. All of the fresh assemblies are used multiple times, as are some of the once-burnt assemblies. The most commonly changed assemblies are fp4 and 1-D, suggesting that there could be PPF problems in these assemblies, which are neighbouring each

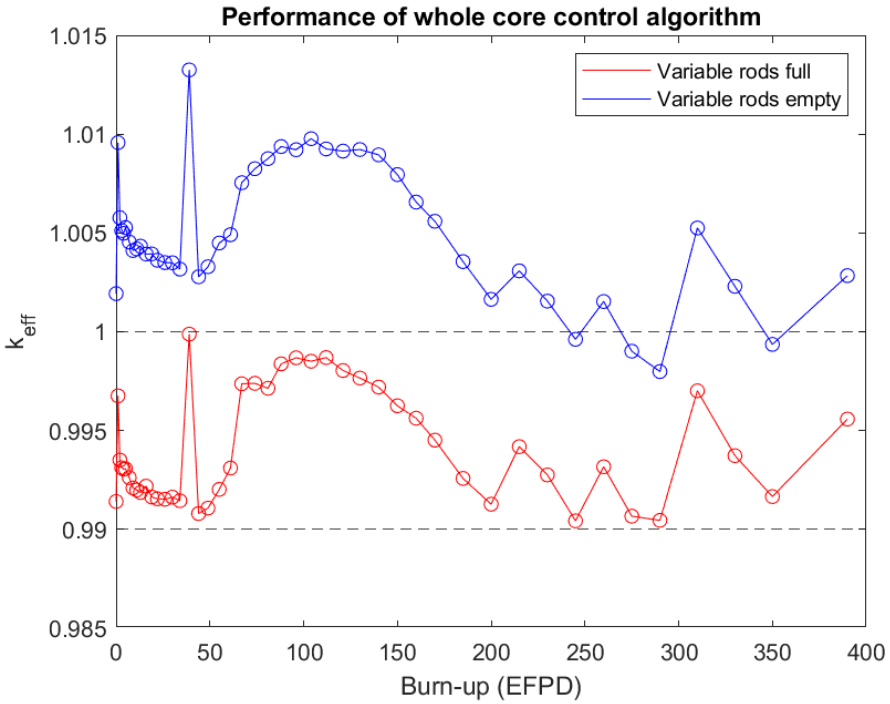


(a) Fixed $1 > k_{\text{eff}} > 0.99$ constraint

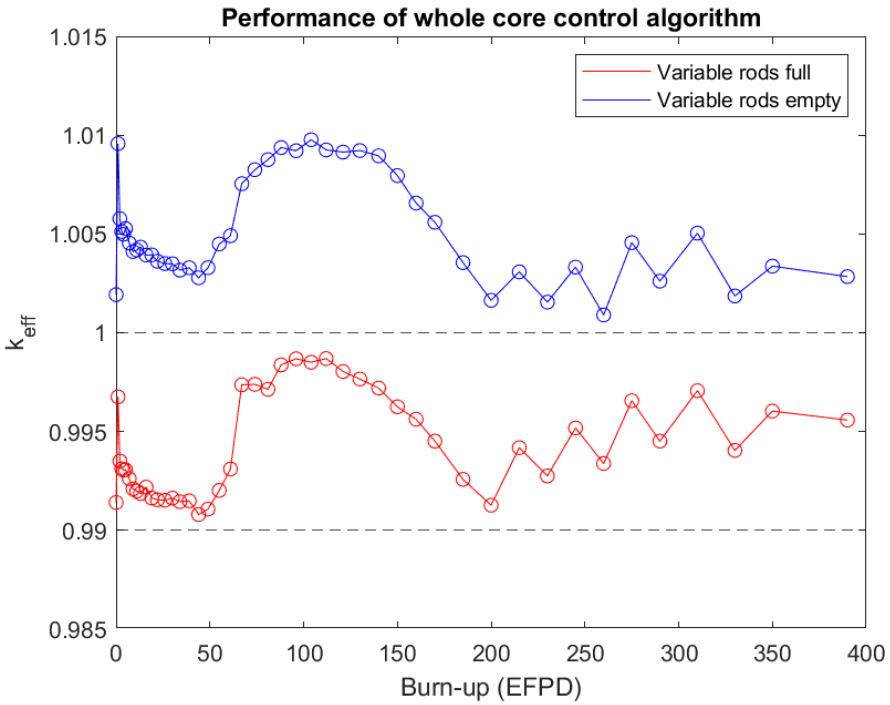


(b) Variable $k_{\text{eff}}$ constraint

Fig. 4.3 Reactivity control achieved during burn-up

other, as they are often altered to change the power distribution. As all fresh assemblies are changed multiple times, this suggests they are not only emptied to provide reactivity control, but are also changed due to PPF values, suggesting that the poison loading could be improved.

### 4.3.3 PPF Animation

Figure 4.5 shows the assembly PPF values and the control tube states at the start-of-cycle. An animation is available on YouTube which has the same figure plotted for each stage of burn-up. The colour map limit is fixed at 1.5 to denote that this is the limit set by the algorithm. The algorithm was able to control PPF < 1.5 at all but 1 burn-up steps, as if the algorithm could not find a solution satisfying the PPF limit after 4 attempts, it moved on to the next burn-up step to conserve resources. It is worth noting that the animation frame indexing starts at step 0, and that between steps 1-15, there are no binary control tube state changes, due to the flat burn-up profile provided by the poison loading.

The one burn-up point where the PPF limit was exceeded was at 350 EFPD, where assembly fp-V, a variable tube, had a PPF of 1.52. This is during the penultimate step, where there is not much excess reactivity in the system, and the variable tubes have had their control authority reduced by burn-up, meaning it is hard for the algorithm to find a solution that satisfies both the $k_{\text{eff}}$ and PPF constraints. The value of 1.52 could be due to error, as the 3 assemblies in symmetrical positions have a PPF value of below 1.5, and 2 being below 1.4. However, the true PPF value in this location is also likely to be higher than estimated, as the simulation assumes the variable tube is 100% full, when in reality it will be only partially full, in order to fine tune $k_{\text{eff}}$, meaning its power will be higher. This assumption that the variable tubes are always full during burn-up also results in the control authority of the variable tubes decreasing faster than expected, as in reality the tubes would absorb less neutrons.

Overall, despite the simplicity of the control algorithm, it has been able to control reactivity at every point in burn-up, as well as controlling PPF to a specified limit at 45/46 burn-up steps. This approximates a maximum bound on the core PPF and variable control needed, as a more complex algorithm that could control each tube separately from the other 8 in the same assembly, could fine tune $k_{\text{eff}}$ better, as well as distribute the power more uniformly across the core.

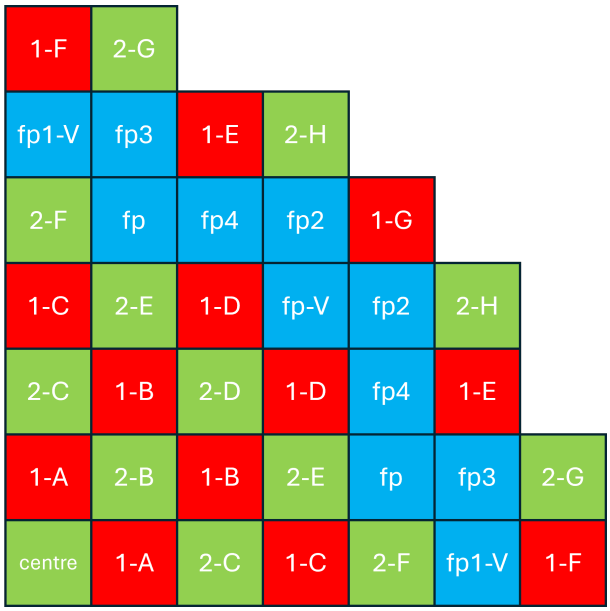


(a) Label for each control tube bank

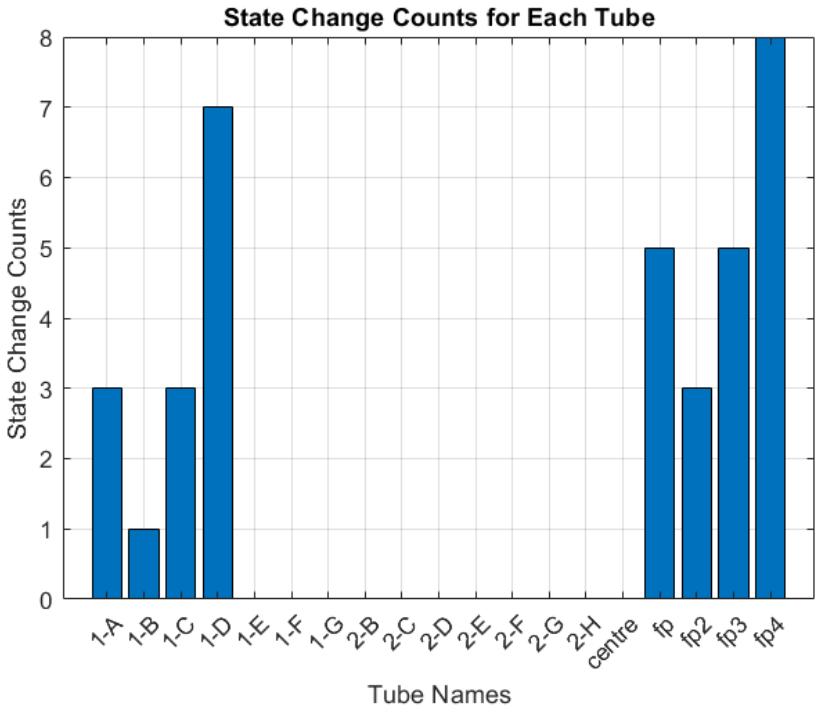


(b) Number of times each tube changes state

Fig. 4.4 Control tube utilisation statistics

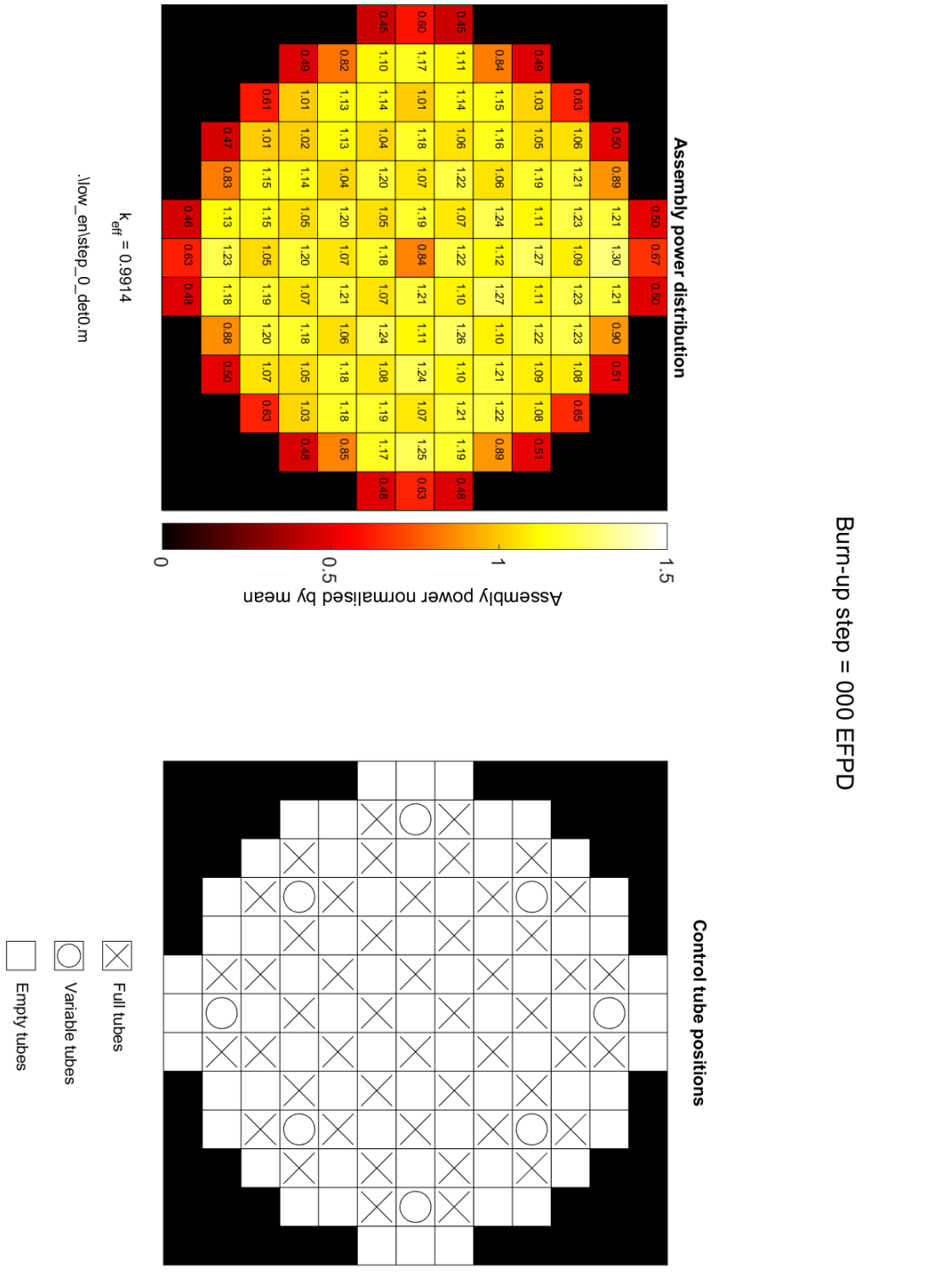


Fig. 4.5 Normalised assembly PPF and tube states at start-of-cycle

# Chapter 5

# Conclusion and Future Work

## 5.1 Future Work

### 5.1.1 Loading Following

One of the initial aims of the project was to evaluate the S7G's capability to load follow, due to the potential demands on future SMRs in a grid with a high share of nuclear energy. It was thought this may be possible using Serpent's transient simulation capability. This was ultimately not possible for several reasons:

- Time scale - in order to load follow, reactors must be able to undergo daily load cycling of the order of 3-5% of rated power per minute [9]. Serpent transient simulations are typically suitable for millisecond time scales [7], and so lack the capability to capture a complex power evolution.
- Resources - even millisecond transient simulations take much more computing resources than a standard criticality or burn-up simulation, and when combined with the large 3D model, the simulations could take weeks to execute.
- During load following, the neutronics of the reactor, which Serpent models, are not the only significant effect, as heat transfer and temperature fluctuations play a large part in controlling the transient behaviour and avoiding sudden power spiking, due to the Doppler effect. Therefore, a coupled thermal-hydraulics/neutronics simulation would be more appropriate for load following, and further work could be done using a different simulation environment.

### 5.1.2 Safety & Economic Case

The PPF analysis in this project focused on the assembly-wise PPF values, and the standard limit of 1.3. However, additional limits exist, such as a pin-wise PPF and nodal PPF, which consider axial power variations within a single pin. Given the control tubes displace multiple pins each, unlike a conventional PWR control rod which displaces one pin, there is the potential for large

power variations within one assembly; therefore more work should be done investigating the pin-wise PPF distribution, which could necessitate a redesign of the poison loading, or variable enrichment schemes.

As discussed in section 3.4.4, conventional PWRs have a negative void coefficient, where if the coolant starts to boil, the decreased moderator density lowers the reactivity of the core. In an S7G reactor, this is not true for the water in the tubes, as if they boil, the decreased water density in the tube decreases the neutron absorption in the tube wall. Therefore, safety case analysis should be carried out for this novel accident case.

One proposed advantage of the S7G is that it does not need soluble boron in order to maintain whole core reactivity control, giving potential cost savings from the equipment needed to manage the boron. In the event of a core melt, one risk for any reactor is recriticality of the corium. Typically this cannot take place, as the fuel cannot become critical without moderation, and the cooling water provided in an emergency has a high boron concentration, meaning it is a net absorber rather than a moderator. Whilst other reactors like the Rolls' SMR do not use soluble boron for whole core control [11], they do have an emergency boron injection system for emergency cooling [12], meaning that the cost of boron management systems cannot be totally offset. Because the lack of soluble boron imposes thickness limits on the control tube walls, there are also negative economic effects associated with not using soluble boron. As seen in section 2.3.1, thicker walls cause a whole core $k_{\text{eff}}$ reduction, which will have negative economic effects, due to operating a shorter fuel cycle. Thicker walls will also necessitate more raw materials, and a higher production cost, albeit this is unlikely to have a large effect due to the relatively cheap price of gadolinium. Therefore, a more thorough economic analysis of the S7G, and of choosing to not use soluble boron, could be conducted.

### 5.1.3 Modelling assumptions and parameters

There are various parts of the project which could be rerun to improve the accuracy of the results, that were not done due to constraints on time and resources. These include:

#### Pre-burnt material compositions

The material compositions of the once-burnt and twice-burnt batches were taken at 492 EFPD, as this was the cycle length suggested by the partial reactivity model when considering the $k_{\text{eff}}$ of an infinite lattice. The actual cycle length of the 3D core with control was only 400 EFPD, therefore the actual material composition after one or two cycles would not be the same as predicted. The batch material compositions could be recalculated using a fuel cycle length of 400 EFPD, which would then give a longer whole core cycle length, due to the decreased burn-up and higher reactivity of the once and twice-burnt batches. In this way, the actual cycle length could be converged upon, somewhere between 400-492 EFPD.

### Control burn-up sequence parameters

During the control algorithm simulations, each simulation was executed with only 200/150 active/inactive cycles, with 100,000 neutrons per generation. Increasing the number of active cycles would decrease the error (5%), so that high PPF values would be less prone to error, and would more reliably reflect the actual power distribution. The algorithm could also be run for more iterations at the burn-up step where it was unable to satisfy the PPF limit, as if it could not find a solution within 4 attempts, it moved on, despite a solution possibly existing. The control algorithm could also be expanded to write new material input files for each burn-up step, in order to adjust the temperature to reflect the reported power, and find a better estimate of the actual PPF values. The height of water necessary in the variable tubes to control reactivity could also be estimated from the control curve, and this height could be used when depleting the core and calculating the PPF values.

### Geometry definitions

The geometry could be expanded to allow the individual operation of each of the 9 tubes per assembly. Structural components such as the assembly spacer grids could also be modelled, to improve the accuracy of $k_{\text{eff}}$.

### Evaluation of key operating points

The reactor behaviour at key operating points (i.e. cold zero, hot zero, hot full power) were calculated for both start and end-of-cycle; however, the end-of-cycle burn-up state was calculated under no control. These points could be re-evaluated using the material compositions from the last step of the control algorithm.

### Tube wall redesign

The current tube walls burn out after one cycle and need replacing. Whilst it was shown that walls twice as thick could last 3 cycles, albeit with a reduction in $k_{\text{eff}}$ when filled with water, it was not established whether this $k_{\text{eff}}$ reduction is also present when the tubes are filled with nitrogen, especially when filled with nitrogen after having been filled with water for the majority of the cycle, which would reflect the operating point at the end of the cycle, which is pertinent when calculating the viable cycle length.

### Poison redesign

The poison burn-up profile was not flat for the first cycle length, and the initial reduction of $k_{\text{eff}}$ was too large. Redesigning the poison loading, and the burn-up profile to be more flat, could help control the PPF values, especially in the assemblies that were found to be the most challenging PPF-wise in section 4.3.

## 5.2 Conclusion

This report has successfully shown how to create a 3D model of a three-batch S7G reactor, which had not previously been done in the public domain, using Serpent. Key operating points of the reactor have been evaluated at both start and end-of-cycle conditions, and the reactor satisfies criticality requirements for Hot Zero and Cold Zero Power.

A simple control algorithm has been designed, that is able to control $k_{\text{eff}}$ to be approximately equal to 1 for all points of burn-up, with fine tuning being possible given additional computational resources. This control has been achieved with only 8 variable level tubes out of 121, and without the use of soluble boron, which could provide economic advantages for a commercial SMR. The assembly-wise power distribution has also been considered, and the algorithm is capable of controlling this to a specified limit of 1.5, although more complex temperature modelling would be needed to ensure this remains below 1.3 for a physical system.

Key design points such as the height and power of the S7G reactor were matched to the Rolls' SMR to allow easy comparison between the two technologies. The average discharge burn-up was 52MWd/kg, which was lower than the three-batch burn-up predicted for the reactor in the previous work, of 65.22 MWd/kg, but brings the burn-up in line with the safety limits on Zircaloy-4 cladding, which stipulate a maximum burn-up of 62 MWd/kg [16]. This is lower than the Rolls' SMR burn-up, of 55-60 MWd/kg, and may be due to increased parasitic absorption in the control tubes, the harder neutron spectrum of the core, and the displacement of many fuel pins in the lattice, despite the higher enrichment. The control worth curve was found to be highly asymmetric, unlike the symmetric S-curve of a PWR.

As discussed in the previous work, the gadolinium tube burnout remains a limiting factor for the design of S7G lattices, with the 3D-model indicating a need to replace them after each fuel cycle. Further work could revisit the lattice design to optimise their thickness, and it has been showed that a doubling of the thickness would extend their life to three fuel cycles, but that with the current control algorithm, all tubes are only filled for a maximum of two cycles during steady-state operation. The rate of photon and neutron energy deposition directly in the control tube water has been identified as another critical safety limit which is novel to the S7G. This has been calculated as 0.36% of thermal power for an average-power assembly, giving a heating power of 42.3kW, which is enough to boil all of the tube water in 6.3 minutes.

Key safety cases, such as a loss of coolant accident, which could drain the control tubes of their water, and a loss of power accident, which could lead to the boiling off of the control tube water due to a loss in circulation, have been identified as having potentially different responses compared to a conventional PWR. The analysis of these accidents, as well as the evaluation of the S7G control for use in load following, remain areas for future work. The use of a neutron-transport code such as Serpent was insufficient for their analysis, due to the lack of temperature variation modelling; therefore future work should seek to use a coupled thermal-hydraulics/neutronics simulator.

# References


[1] ANSWERS Software (2023). WIMS. [online] https://answerssoftwareservice.com/wims/.

[2] Dalle, H. M., de Mattos, J. R. L., and Dias, M. S. (2013). Enriched Gadolinium Burnable Poison for PWR Fuel – Monte Carlo Burnup Simulations of Reactivity. In Mesquita, A. Z., editor, *Current Research in Nuclear Reactor Technology in Brazil and Worldwide*, chapter 4. IntechOpen, Rijeka.

[3] Driscoll, M., Downar, T., and Pilat, E. (1990). *The Linear Reactivity Model for Nuclear Fuel Management*. American Nuclear Society.

[4] Evans, J. A., DeHart, M. D., Weaver, K. D., and Keiser, D. D. (2022). Burnable absorbers in nuclear reactors – a review. *Nuclear Engineering and Design*, 391:111726.

[5] Kamenov, K. (2003). Application of the SPPSHB computer code system for fuel loading of assemblies from cores of units 1 and 2 to cores of units 3 and 4 at Kozloduy NPP. [online] https://inis.iaea.org/collection/NCLCollectionStore/_Public/36/040/36040500.pdf.

[6] Lawrence, J. (2022). Modelling the S7G Reactor. MEng project report. University of Cambridge.

[7] Leppänen, J., Pusa, M., Viitanen, T., Valtavirta, V., and Kaltiaisenaho, T. (2015). The Serpent Monte Carlo code: Status, development and applications in 2013. *Annals of Nuclear Energy*, 82:142–150.

[8] Lindley, B., Wilkinson, P., Couet, A., and Shahrokhi, F. (2022). Telescopic control rod for significant reduction in HTR height and cost. *Annals of Nuclear Energy*, 169:108953.

[9] Lokhov, A. (2011). Load-following with nuclear power plants. *NEA News*, 29.2:18–22.

[10] Parks, G. (2024). 4M16 Fuel Management Handout.

[11] Rolls-Royce (2019). UK SMR (Rolls-Royce and Partners). [online] https://aris.iaea.org/PDF/UK-SMR_2020.pdf.

[12] Rolls Royce SMR (2023). E3S Case Chapter 24: ALARP Summary. [online] https://gda.rolls-royce-smr.com/assets/documents/documents/rr-smr-e3s-case-chapter-24---alarp-summary-issue-1.pdf.

[13] Serpent Wiki (2024). Serpent Input Syntax Manual. [online] https://serpent.vtt.fi/mediawiki/index.php/Input_syntax_manual#set_edepmode.

[14] Tsvetkov, P. (2011). *Nuclear Power: Deployment, Operation and Sustainability*. IntechOpen.

[15] United States Nuclear Regulatory Commission (2021). Reflector. [online] https://www.nrc.gov/reading-rm/basic-ref/glossary/reflector.html.

[16] Westinghouse Electric Company LLC (2017). Non-LOCA Accidents. [online] https://www.nrc.gov/docs/ML0132/ML013270095.pdf.

[17] World Nuclear Association (2017). Nuclear Power Economics and Project Structuring. [online] https://world-nuclear.org/our-association/publications/online-reports/nuclear-power-economics-and-project-structuring.aspx.

[18] World Nuclear Association (2021). Nuclear Fuel and its Fabrication. [online] https://world-nuclear.org/information-library/nuclear-fuel-cycle/conversion-enrichment-and-fabrication/fuel-fabrication.aspx.

[19] World Nuclear Association (2023). Nuclear Power Reactors. [online] https://www.world-nuclear.org/information-library/nuclear-fuel-cycle/nuclear-power-reactors/nuclear-power-reactors.aspx.

# Appendix A

# Appendices

## A.1 Risk Assessment Retrospective

As a 100% computational-based project, the main risks stemmed from bad computer use practices, such as straining of the eyes and muscles due to bad posture. To avoid these, lights were kept on whilst working, and my computer was set permanently to 'night mode', in order to reduce the blue light emitted. Regular breaks were taken, and my desk chair and desk set-up were well adjusted. As a result, I have experienced no negative health effects.

## A.2 Geometry Files

The Serpent input geometry files, as well as relevant scripts, such as the Python script used for the control algorithm, are available on the University Sharepoint.